Assessing the impact of stratospheric aerosol injection on U.S. convective weather environments

Ivy Glade[1], James Wilson Hurrell[1], Lantao Sun[1], and Kristen Rasmussen[1]

[1]Colorado State University

August 22, 2023

Abstract

Continued climate warming, together with the overall evaluation and implementation of a range of climate mitigation and adaptation approaches, has prompted increasing research into proposed solar climate intervention (SCI) methods, such as stratospheric aerosol injection (SAI). SAI would use aerosols to reflect a small amount of incoming solar radiation away from Earth to stabilize or reduce future warming due to increasing greenhouse gas concentrations. Research into the possible risks and benefits of SAI relative to the risks from climate change is emerging. There is not yet, however, an adequate understanding of how SAI might impact human and natural systems. For instance, little to no research to date has examined how SAI might impact environmental conditions critical to the formation of severe convective weather over the United States (U.S.). This study uses ensembles of Earth system model simulations of future climate change, with and without hypothetical SAI deployment, to examine possible future changes in thermodynamic and kinematic parameters critical to the formation of severe weather during convectively active seasons over the U.S. Results show that simulated forced changes in thermodynamic parameters are significantly reduced under SAI relative to a no-SAI world, while simulated changes in kinematic parameters are more difficult to distinguish. Also, unforced internal climate variability is likely to significantly modulate the projected forced climate changes over large regions of the U.S.

Assessing the impact of stratospheric aerosol injection on U.S. convective weather environments

Ivy Glade[1]**, James W. Hurrell**[1]**, Lantao Sun**[1]**, Kristen L. Rasmussen**[1]

[1]Department of Atmospheric Science, Colorado State University, Fort Collins, CO, USA

Key Points:

- SAI may prevent future increases in the magnitude of thermodynamic parameters relevant to the formation of severe weather over the U.S.
- Future changes in wind shear, a kinematic parameter, is driven largely by changes in tropical precipitation whether or not SAI is deployed.
- Internal decadal-scale climate variability is likely to impact future projections of regional changes in convective weather environments.

Corresponding author: Ivy Glade, `ivyglade@rams.colostate.edu`

Abstract

Continued climate warming, together with the overall evaluation and implementation of a range of climate mitigation and adaptation approaches, has prompted increasing research into proposed solar climate intervention (SCI) methods, such as stratospheric aerosol injection (SAI). SAI would use aerosols to reflect a small amount of incoming solar radiation away from Earth to stabilize or reduce future warming due to increasing greenhouse gas concentrations. Research into the possible risks and benefits of SAI relative to the risks from climate change is emerging. There is not yet, however, an adequate understanding of how SAI might impact human and natural systems. For instance, little to no research to date has examined how SAI might impact environmental conditions critical to the formation of severe convective weather over the United States (U.S.). This study uses ensembles of Earth system model simulations of future climate change, with and without hypothetical SAI deployment, to examine possible future changes in thermodynamic and kinematic parameters critical to the formation of severe weather during convectively active seasons over the U.S. Results show that simulated forced changes in thermodynamic parameters are significantly reduced under SAI relative to a no-SAI world, while simulated changes in kinematic parameters are more difficult to distinguish. Also, unforced internal climate variability is likely to significantly modulate the projected forced climate changes over large regions of the U.S.

1 Introduction

Global carbon dioxide (CO_2) emissions have increased every decade since the 1960s and are projected to continue to increase over at least the next several decades (Friedlingstein et al., 2022; Jiang & Guan, 2016; Peters et al., 2012). It is therefore very unlikely that global climate warming will be limited to 1.5 or even 2°C above pre-industrial temperatures unless action is taken soon to drastically reduce emissions (IPCC, 2021). In fact, climate warming is projected to be over 2°C by the end of the century under moderate and current policy-relevant emissions scenarios, surpassing what is considered to be a safe threshold of warming (IPCC, 2021; Riahi et al., 2017; UNEP, 2022). Climate impacts such as drought intensification (Mukherjee et al., 2018; Strzepek et al., 2010), increases in extreme precipitation (M. R. Allen & Ingram, 2002; Donat et al., 2016; Dougherty & Rasmussen, 2020; Prein et al., 2017) and continued sea ice loss (Stroeve et al., 2012) are projected to worsen over the coming decades (IPCC, 2021). Future changes also include the potential for increases in the frequency and intensity of severe convective weather over large portions of the United States (U.S.) (Diffenbaugh et al., 2013; Hoogewind et al., 2017; Lepore et al., 2021; K. L. Rasmussen et al., 2017; Seeley & Romps, 2015; Tippett et al., 2015; Trapp et al., 2007, 2009, 2019).

Given slow progress toward reducing fossil fuel emissions and the urgency to limit continued temperature warming, the U.S. National Academies of Science, Engineering and Medicine (NASEM) recently recommended the formation of a transdisciplinary research program to identify the potential benefits and risks of solar climate intervention (SCI) relative to the risks posed by climate change (NASEM, 2021). Most SCI approaches would cool the planet by reflecting a small amount of incoming solar radiation away from Earth, potentially minimizing some of the worst consequences of anthropogenic climate change while buying more time for mitigation and the deployment of CO_2 removal technologies. Stratospheric aerosol injection (SAI) is one proposed form of SCI that would involve, perhaps, the injection of sulfur dioxide (SO_2) into the stratosphere, which would react with hydrogen and oxygen to form highly reflective sulfate aerosols (Crutzen, 2006; Rasch et al., 2008; Richter et al., 2022).

Several Earth-system models have been used to simulate a future climate with SAI under different climate change scenarios (Kravitz et al., 2011; Richter et al., 2022; Tilmes et al., 2018; Visioni et al., 2023). Research to date has included examining changes in global and regional temperature and precipitation (Hueholt et al., 2023; Richter et al., 2022; Tilmes et al., 2018), atmospheric circulation patterns (Bednarz et al., 2022), extreme temperature and precipitation events (Barnes et al., 2022; Ji et al., 2018), and ecological responses (Zarnetske et al., 2021), in addition to potential deployment technologies (Lockley et al., 2022; Smith & Wagner, 2018). Such studies have demonstrated that SAI could potentially be deployed to stabilize or reduce global mean temperature to a specific temperature target (Richter et al., 2022; Tilmes et al., 2018; Visioni et al., 2021); however, research has also indicated that regional impacts of SAI could be both positive and negative. For example, major African river basins may have enhanced drought risk because SAI is projected to cause precipitation decreases that overcompensate for projected increases due to climate warming (Abiodun et al., 2021). On the other hand, future projections indicate that SAI has the potential to reduce Greenland ice sheet mass loss (Moore et al., 2019) and minimize the loss of Arctic sea ice (Lee et al., 2023).

While research on the potential impacts of SAI has been increasing and broadening in recent years, current research remains scattered and ad hoc, so a holistic understanding of how SAI would impact Earth and human systems is limited (NASEM, 2021). For instance, while there have been studies documenting the impact of climate change on the large-scale environments in which severe weather (as defined by Galway, 1989) forms (Diffenbaugh et al., 2013; Franke et al., 2023; Hoogewind et al., 2017; Lepore et al., 2021; K. L. Rasmussen et al., 2017; Seeley & Romps, 2015; Trapp et al., 2007, 2009; Chen et al., 2020), there are no studies that have examined the potential impact of SAI on those environments. The topic is of relevance given increasing economic impacts and more frequent billion dollar U.S. severe weather disasters in recent decades (NCEI, 2022).

Large-scale parameters and proxies have been used to identify what environmental conditions are favorable to the formation of severe weather, largely in order to improve short-term predictability and overcome discontinuities and inconsistencies in limited observational records (e.g., Doswell et al., 1996; E. N. Rasmussen & Blanchard, 1998; Brooks et al., 2003; Craven & Brooks, 2004). More recently, such parameters and proxies have also been used to predict how the behavior of severe weather might change on longer time scales, such as through the end of the century (e.g., Diffenbaugh et al., 2013; Franke et al., 2023; Hoogewind et al., 2017; Lepore et al., 2021; K. L. Rasmussen et al., 2017; Trapp et al., 2007). In part, this is because integrating convection-permitting models over long periods of time is computationally expensive, and these parameters and proxies are resolvable using coarser resolution Earth-system models.

Parameters commonly analyzed include convective available potential energy (CAPE), convective inhibition (CIN), and the wind shear from the surface to $\sim$6 km (S06). With climate change, the magnitudes of both CAPE and CIN are projected to increase in the U.S. east of the Rocky Mountains in both the spring and summer (Diffenbaugh et al., 2013; Franke et al., 2023; Hoogewind et al., 2017; Lepore et al., 2021; K. L. Rasmussen et al., 2017; Trapp et al., 2007; Chen et al., 2020). Increases in the magnitude of CAPE and CIN have been attributed to increases in temperature and moisture throughout the troposphere (K. L. Rasmussen et al., 2017, see also Fig. S2) and decreases in low-level relative humidity (Chen et al., 2020). Wind shear (S06) is also generally projected to decrease in both the spring and summer seasons across the U.S., especially east of the Rockies (Trapp et al., 2007; Hoogewind et al., 2017; Lepore et al., 2021), a change that largely reflects decreases in the zonal wind at ∼6 km (Diffenbaugh et al., 2013; Franke et al., 2023).

Combined proxies that consider the integrated effects of more than one convective weather environment parameter have also been analyzed (Diffenbaugh et al., 2013; Hoogewind et al., 2017; Lepore et al., 2021; Seeley & Romps, 2015; Trapp et al., 2007, 2009). Proxies that consider both the thermodynamic and kinematic characteristics of the environments have been shown to better discriminate between environments conducive to ordinary thunderstorms, supercells, and tornadic supercells than individual thermodynamic or kinematic parameters alone (E. N. Rasmussen & Blanchard, 1998). CAPES06, defined as the product of CAPE and S06, has been used to distinguish significant severe storms from those that are less severe (Brooks et al., 2003; E. N. Rasmussen & Blanchard, 1998). This proxy is often used in tandem with other convective weather environment parameters to describe whether an environment is favorable to the formation of severe weather on a given day (Diffenbaugh et al., 2013; Hoogewind et al., 2017; Lepore et al., 2021; Seeley & Romps, 2015; Trapp et al., 2007). The number of days with high magnitude CAPES06 are projected to increase with future warming across the eastern U.S. (Seeley & Romps, 2015). Diffenbaugh et al. (2013) suggests that CAPES06 is expected to increase across the eastern U.S. even though S06 is projected to decrease, because decreases in S06 are expected to occur on days when CAPE is already low.

Previous research examining projections of convective weather environments has mostly considered high emissions trajectories that are not consistent with current climate policies. In this study, the potential impact of climate warming on convective weather environments in the U.S. is examined using a 10-member ensemble of Earth-system model simulations under the Shared Socioeconomic Pathway 2-4.5 (SSP2-4.5) emissions scenario. This is a "middle of the road" scenario more consistent with current climate policies. It projects ∼2.7°C of global warming by the end of the century (O'Neill et al., 2017) and considers the slow development and deployment of sustainability practices such as CO_2 emissions reduction and removal technologies (IPCC, 2021; Riahi et al., 2017). In addition, parallel climate change integrations with a hypothetical SAI deployment are analyzed to document the potential impact of SAI on large-scale convective weather environments, relative to the impacts from climate change alone. To our knowledge, this is the first study to examine the potential influence of SAI on future convective weather environments.

2 Methodology

2.1 Model Information

This study utilizes a set of parallel simulations of climate change with and without SAI; specifically, the Assessing Responses and Impacts of Solar climate intervention on the Earth system using stratospheric aerosol injection (ARISE-SAI; Richter et al., 2022). These simulations were performed using the freely available Community Earth System Model version 2 (CESM2), a fully coupled model with the Whole Atmosphere Community Climate Model version 6 (WACCM6) as the atmospheric component (Danabasoglu et al., 2020; Gettelman et al., 2019). WACCM6 is a high-top model with a well-represented stratosphere that includes 70 vertical levels with a model top of 4.5x10^{-6} hPa ($\sim$130 km) and a horizontal resolution of 1.25° longitude and 0.9° latitude (Danabasoglu et al., 2020). ARISE-SAI consists of two 10-member ensembles of climate change with and without SAI. Both ensembles follow the moderate SSP2-4.5 emissions scenario (O'Neill et al., 2017). The ARISE-SAI climate change simulations consist of five members that run from 2015-2100 and were carried out as a part of the Coupled Model Intercomparison Project Phase 6 (Eyring et al., 2016). Five other ensemble members cover the period from 2015-2069 and were branched off from three existing historical CESM2-WACCM6 simulations (1850-2014) with the addition of a small temperature perturbation at the first model time step (Richter et al., 2022).

The first five members of the ensemble with a hypothetical SAI deployment were initialized in 2035 using the first five members of the climate change (SSP2-4.5) ensemble. The last five members were initialized in a similar way, but with the addition of a small temperature perturbation (Richter et al., 2022). Each of the 10 SAI simulations extend through 2069, with SO_2 being injected into the stratosphere continuously beginning in 2035 in order to maintain global mean temperature at $\sim$1.5°C above its pre-industrial value. In addition, the ARISE-SAI injection strategy is designed to maintain the equator-to-pole and interhemispheric temperature gradients to values consistent with those observed at the 1.5°C temperature target (Kravitz et al., 2017; MacMartin et al., 2014; Richter et al., 2022). The stabilizing influence of SAI is clear when examining not

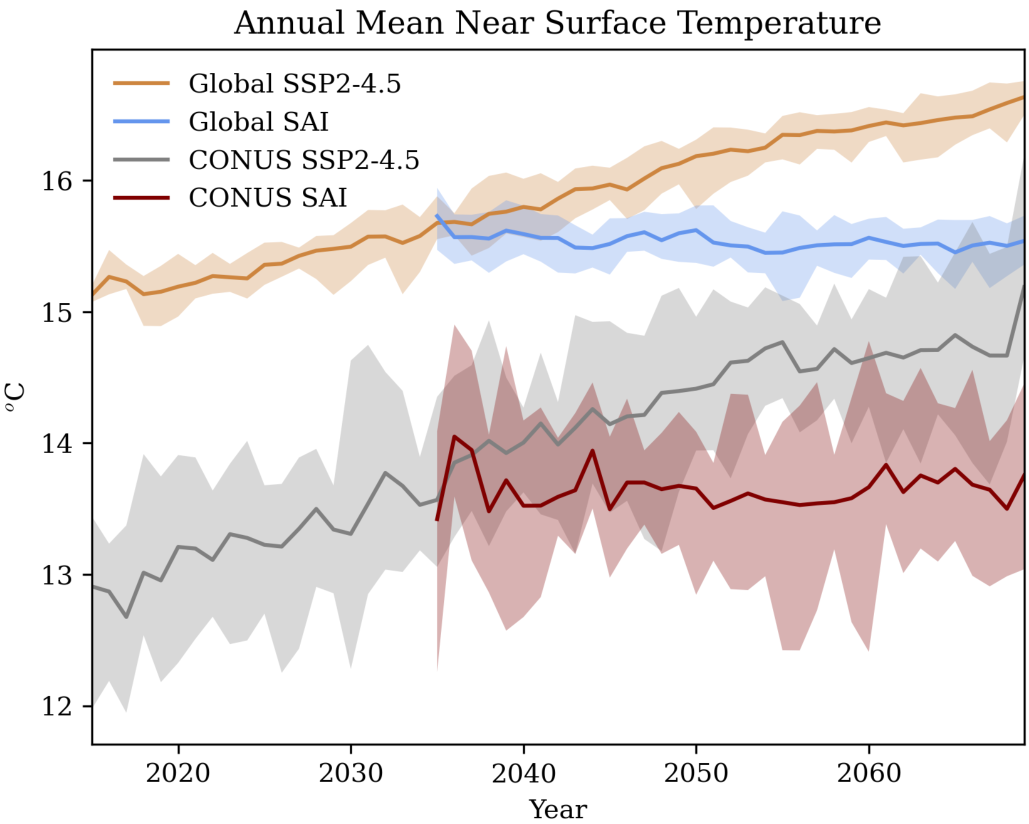

Figure 1: Annual mean near-surface (2 m) temperature from the SSP2-4.5 simulations (2015-2069) and the simulations where SAI is deployed (2035-2069). Results averaged over the globe are given by the tan (SSP2-4.5) and blue (SAI) lines, while those averaged over the contiguous U.S. are given by the gray (SSP2-4.5) and red (SAI) lines. Ensemble means are shown by the thick solid lines, while the minimum and maximum ranges of the individual ensemble members are shown by the corresponding color shading.

only the time series of global 2 m temperature change (Hueholt et al., 2023; Richter et al., 2022), but also that for the contiguous U.S (CONUS) (Figure 1).

2.2 Convective Weather Environment Parameters and Proxies

CAPE (J kg^{-1}) and CIN (J kg^{-1}) are thermodynamic parameters which consider the temperature and moisture content of the atmosphere (Doswell & Rasmussen, 1994). CAPE is a measure of potential energy that is defined by the vertical integral of buoyancy from the level of free convection to the equilibrium level, and is analogous to updraft velocity (Doswell & Rasmussen, 1994; E. N. Rasmussen & Blanchard, 1998; Trapp et al., 2007). CIN represents the negative buoyancy and is indicative of the potential to suppress convective motions (E. N. Rasmussen & Blanchard, 1998). CAPE and CIN were calculated as the most-unstable parcel in the lowest 3000 m of the atmosphere (MUCAPE and MUCIN), which is a useful method for capturing cases of elevated instability, while being effective at identifying low-level or surface-based instability when present (Doswell & Rasmussen, 1994).

S06 (m s^{-1}) is a kinematic parameter that is representative of the change in the horizontal wind vector from $\sim$10 m above ground-level to approximately 6 km altitude. This measure of wind shear is used to diagnose whether or not an environment is favorable to the formation of significant severe thunderstorms (Brooks et al., 2003; E. N. Rasmussen & Blanchard, 1998). In particular, small magnitudes of S06 are typically associated with the development of relatively small, short-lived single-cell thunderstorms, while larger magnitudes of S06 are typically associated with the potential for development of supercell thunderstorms, which are longer-lived, more organized, and more intense (Weisman & Klemp, 1982).

The combination of CAPE and 0-6 km wind shear (CAPES06; m^3 s^{-3}) is a good discriminator for significant severe thunderstorm events (Brooks et al., 2003; Marsh et al., 2007; E. N. Rasmussen & Blanchard, 1998; Trapp et al., 2007). CAPES06 is considered simply as the product of CAPE and S06. Some previous studies have weighted S06 more heavily than CAPE (Brooks et al., 2003; Seeley & Romps, 2015), but Seeley and Romps (2015) note that varying the weight of S06 in calculations of CAPES06 did not have a large impact on future projections of favorable convective weather environments.

While results are presented as spatial maps over the CONUS, area-averaged statistics over the Southeast and Midwest regions are also computed. The Southeast is defined as the grid points bounded by 39°-48°N and 255°-274°W, while the Midwest is defined as the region within 30°-39°N and 255°-280°W (Figure S1). While all seasons and other regions over the U.S. were examined, the analysis here is restricted to the Southeast region during the boreal spring season (MAM) and the Midwest region during the boreal summer season (JJA). These regions and seasons were chosen subjectively based on the climatological seasonal distributions of both convective weather environments and severe weather events (e.g., Kelly et al., 1985; Doswell et al., 2005; Brooks et al., 2007; Taszarek et al., 2020). The representation of convective weather environments in both the Community Atmosphere Model version 6 (CAM6) (Danabasoglu et al., 2020), an atmosphere only model, and CESM2-CAM6, a fully coupled Earth-system model, have been validated against the fifth generation of the high resolution global reanalysis dataset produced by ECMWF (ERA5) (Franke et al., 2023; Li et al., 2020; Chen et al., 2020). CAM6 is the low-top version of WACCM6, where the two models have the same vertical structure up to 87 hPa and nearly identical parameterizations (Danabasoglu et al., 2020). These validations have shown that both CAM6 and CESM2-CAM6 are able to well represent convective weather environments over the eastern CONUS, as well as the synoptic features (Li et al., 2020) and the influence of large-scale modes of variability, such as the El Niño Southern Oscillation (ENSO; Franke et al., 2023).

Most previous studies that have considered convective weather environment parameters have calculated these indices using model output at 00 Z, which is known to represent the time when MUCAPE is maximized in the central to eastern U.S. (e.g., Trapp et al., 2007; Diffenbaugh et al., 2013; Seeley & Romps, 2015). However, only daily mean data are available for all 10 of the ARISE-SAI ensemble members. To assess the suitability of using daily averaged data, 00 Z data were extracted from one ensemble member from the CESM2 Large Ensemble (CESM2-LE; Rodgers et al., 2021) and results were compared to those computed from the daily averaged data from the same simulation. The CESM2-LE is a 100-member ensemble that runs from 1850-2100 and follows the SSP3-7.0 emissions scenario, which warms more and has slower development of mitigation and adaptation practices relative to SSP2-4.5 (O'Neill et al., 2017). The CESM2-LE utilizes the low-top atmospheric component of CESM2 (CAM6; Rodgers et al., 2021).

The time evolutions from 2015-2069 of MUCAPE, MUCIN, S06, and CAPES06 computed at 00 Z were compared to those computed as a daily mean quantity. The analysis was based on anomalies relative to 2015-2034 climatologies. The time evolution of CAPES06 anomalies for the Southeast in MAM and the Midwest in JJA indicates high correlation between the sub-daily and daily mean anomalies in both regions ($r = 0.988$ and $r = 0.946$) (Figure 2). Correlations between sub-daily and daily mean anomalies are similarly high for MUCAPE, MUCIN and S06 (not shown). Thus, while differences exist in the absolute magnitude of the convective weather environment parameters when computed from sub-daily relative to daily mean data (especially for MUCIN, which is maximized at night rather than in the afternoon due to nocturnal stability in the boundary layer), the

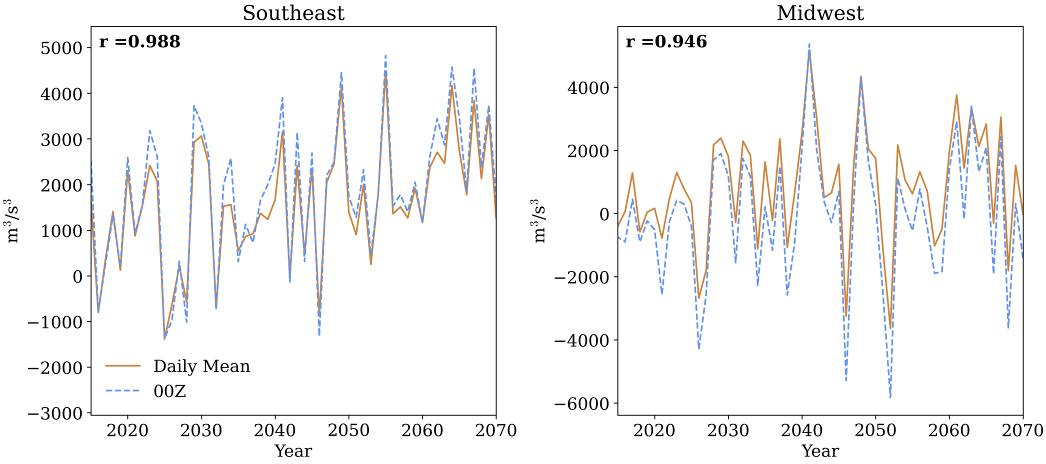

Figure 2: Time series of CAPES06 anomalies in the Southeast in MAM and in the Midwest in JJA from 2015-2070 from one member of the CESM2 Large Ensemble. Anomalies are relative to the 2015-2034 mean. The tan line represents CAPES06 anomalies calculated from daily mean data, while the blue dashed line represents CAPES06 anomalies from 00 Z data only. The correlation between the two time series is the r-value in the top left of each graph.

changes over time of the parameters computed from daily mean data, as well as the differences between the SAI and no-SAI simulations, are very similar to the temporal changes of the parameters computed from 00 Z data only. Using the daily mean data that is available from all 10 ARISE-SAI ensemble members for a better estimation of the forced changes in climate, as well as to better examine how the forced changes might be modified by decadal and multi-decadal internal climate variability.

3 Results

3.1 Forced Responses

Differences in future projections with and without SAI are evident in many convective weather environment parameters averaged over the Southeast and Midwest regions (Figure 3). Without SAI deployment, MUCAPE increases throughout the time period relative to the base period (2015-2034), but with SAI deployment MUCAPE stabilizes (Figure 3a, 3e). Similarly, climate change causes an increase in the magnitude of MUCIN (increasingly negative values) in both regions while SAI stabilizes MUCIN near 2035 levels

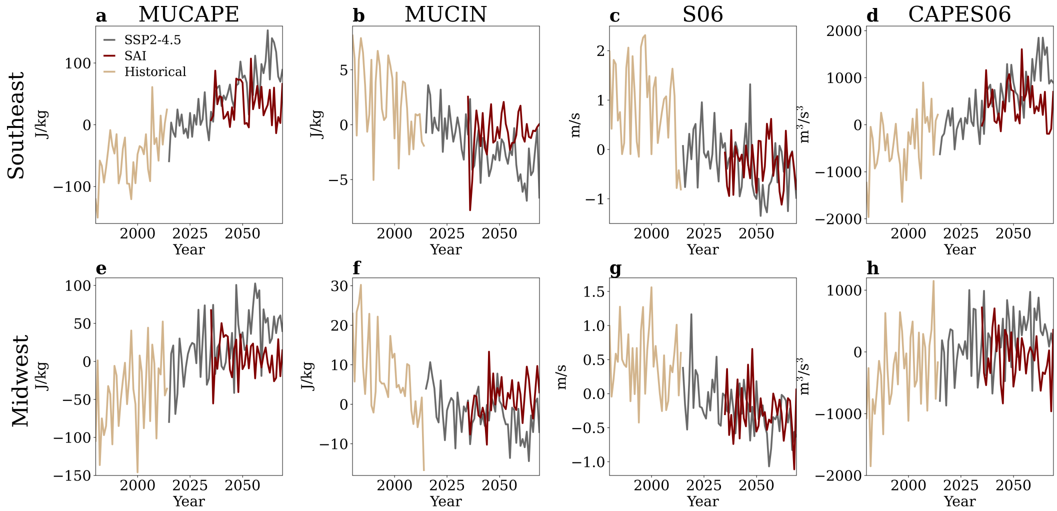

Figure 3: Time series showing MUCAPE (J kg^{-1}) (a and e), MUCIN (J kg^{-1}) (b and f), S06 (m s^{-1}) (c and g), and CAPES06 (m^3 s^{-3}) (d and h) anomalies relative to the 2015-2034 mean for the Southeast in MAM (top row) and the Midwest in JJA (bottom row) from 1980-2069. The tan line represents the three-member ensemble mean from CESM2(WACCM6) historical runs, the gray line represents the 10-member ensemble mean from the SSP2-4.5 simulations, and the red line represents the 10-member ensemble mean from the simulations with SAI deployment beginning in 2035.

in these simulations (Figure 3b, 3f). S06 decreases in magnitude throughout the time period in the no-SAI simulations, but the influence of SAI on wind shear is less clear (Figure 3c, 3g). The sign of future greenhouse-gas induced changes in MUCAPE, MUCIN and S06 are in general agreement with previous studies (Diffenbaugh et al., 2013; Lepore et al., 2021; Trapp et al., 2009; K. L. Rasmussen et al., 2017), although magnitudes differ, partly because earlier studies examined climate change scenarios other than SSP2-4.5 and with a variety of model frameworks. Projected increases in the magnitude of CAPES06, which are dominated by increases in MUCAPE with continued climate warming (Figure 3d, 3h) are also in line with earlier studies (Diffenbaugh et al., 2013; Seeley & Romps, 2015; Trapp et al., 2007). It thus follows that changes in CAPES06 mirror the simulated changes to MUCAPE in the SAI runs, with anomalies stabilizing to approximately 2035 levels (Figure 3d, 3h).

The underlying climatological (2015-2034) spatial distributions of these parameters from the ARISE-SAI simulations (Figure 4) provide context for projected changes with and

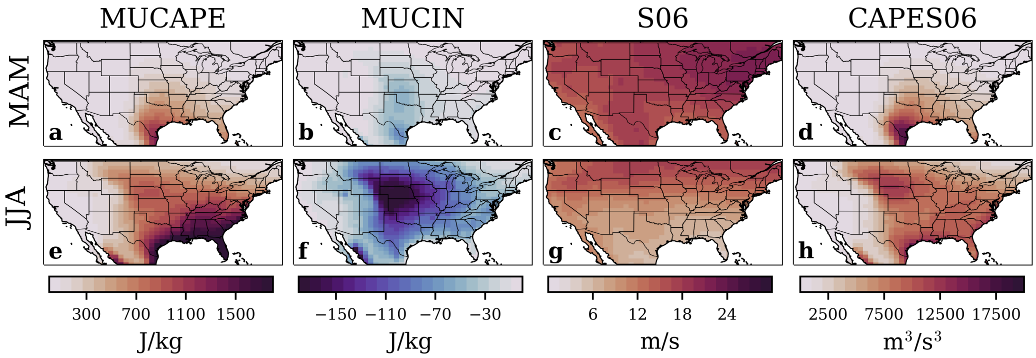

Figure 4: Climatological MUCAPE (a and e), MUCIN (b and f), S06 (c and g) and CAPES06 (d and h) for MAM (top row) and JJA (bottom row) over 2015-2034 for the SSP2-4.5 simulations.

without SAI, and they are in good agreement with observations (e.g., Franke et al., 2023; Li et al., 2020; Chen et al., 2020; K. L. Rasmussen et al., 2017). In MAM, maximum values of MUCAPE are found over the south-central U.S., especially just west of the Gulf of Mexico (Figure 4a). The area of maximum MUCAPE becomes much larger in JJA, with large values generally east of the Rockies and the greatest magnitudes over the far southern U.S. (Figure 4e). The changes between MAM and JJA are especially notable over the Northern Plains and the Midwest, where MUCAPE in the summer has magnitudes near those of the Southeast in MAM (Figure 4e).

Similar to MUCAPE, the magnitude of MUCIN increases greatly from MAM to JJA (Figure 4b, 4f), although again note the magnitudes of the climatological values from daily mean data are larger than in previous studies that have utilized data from the afternoon only. In particular, the largest magnitudes of MUCIN are concentrated over Texas, Oklahoma and Kansas in MAM, but by JJA the largest magnitudes are shifted to the central Great Plains. S06 is positive over the entire U.S. during both seasons, although it is larger in spring than summer (Figure 4c, 4g). In both seasons, maximum values of wind shear are over the northern third of the U.S. The distribution of CAPES06 largely mirrors the distribution of MUCAPE in both MAM and JJA (Figure 4d, 4h), although CAPES06 has a more uniform distribution across the eastern half of the U.S. in JJA compared to MUCAPE (4d, 4h).

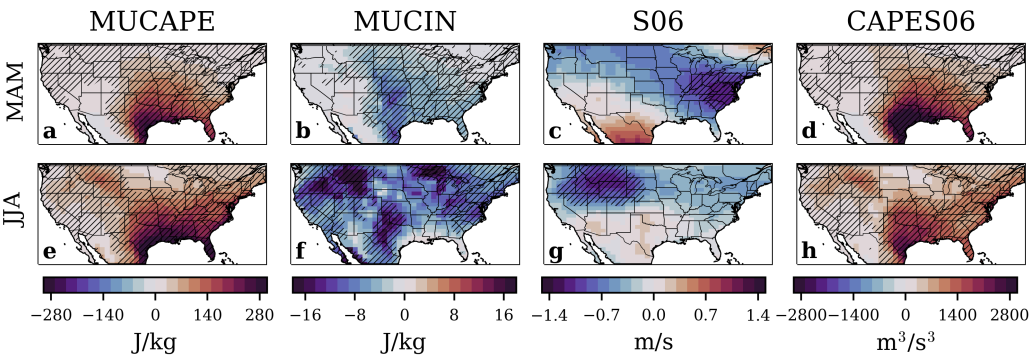

Figure 5: The differences between 2060-2069 (SSP2-4.5) and 2015-2034 (SSP2-4.5) ensemble mean MUCAPE, MUCIN, S06, and CAPES06, in MAM (top row) and JJA (bottom row). Stippling indicates statistical significance at the α=0.05 level.

To examine how climate change affects these environmental parameters, the average changes in the last decade of the ARISE-SAI simulations (2060-2069) are examined relative to the climatological period (2015-2034; Figure 5). In the spring and summer, MUCAPE, MUCIN, and CAPES06 are all projected to increase in magnitude with climate change (Figure 5). Over most regions, these increases are statistically significant at the α=0.05 level for the two-sample t-test (to account for issues related to multiple testing across the U.S. domain, the method outlined in Wilks (2016) was used to control the false discovery rate). Wind shear (S06) is projected to decrease in magnitude during MAM across much of the U.S., with decreases largest in the eastern U.S. (Figure 5c). S06 is also projected to decrease in the summer months, with the largest decreases in the northwest U.S. where convective activity is not as significant historically (Figure 5g). While decreases in wind shear are evident across much of the U.S., the magnitude of the decrease is relatively small compared to the magnitude of the underlying climatology (Figure 4c, 4g, 5c, 5g): climatological S06 values exceed 20 m s^{-1} across much of the U.S., while projected changes by 2060-2069 exceed 1 m s^{-1} over only limited regions (Figure 5c, 5g). Projected increases in MUCAPE, MUCIN and CAPES06, as well as projected decreases in S06, are broadly consistent with previous literature (Diffenbaugh et al., 2013; Franke et al., 2023; Hoogewind et al., 2017; Lepore et al., 2021; K. L. Rasmussen et al., 2017; Seeley & Romps, 2015; Trapp et al., 2007, 2009).

In the SAI simulations, future changes in the magnitudes in MUCAPE, MUCIN and CAPES06 are generally much smaller and less statistically significant across the U.S. (Figure 6) than in the no-SAI simulations (Figure 5). This suggests that if SAI were to be deployed, the convective weather environment parameters analyzed here would not change appreciably from today, although that conclusion may be specific to the ARISE-SAI simulations. Future changes in S06 with SAI, however, are generally similar to those projected in the no-SAI simulations. For instance, the spatial patterns of projected decreases in S06 with SAI are similar to those without SAI in MAM (Figure 5c, 6c), although regions of maximum decrease differ. Since an objective of the ARISE-SAI experiment is to not only keep global average temperature near its 2035 value but also to preserve the equator-to-pole temperature gradient (Richter et al., 2022), it is difficult to simply attribute the S06 decreases in the no-SAI simulations (Figure 5c) to changes in the thermal wind balance, as has been done previously (Trapp et al., 2007; Seeley & Romps, 2015). The results suggest that there could be a different mechanism driving future changes in S06 that has not previously been identified. This aspect is further explored in the Discussion section.

Another way to examine the impacts of SAI on convective weather environment parameters relative to the effects from increasing greenhouse concentrations alone is to directly difference the SAI and no-SAI simulations. Here this is done for differences averaged over the 2060-2069 decade. For MUCAPE, MUCIN, and CAPES06, the differences follow a similar spatial pattern and magnitude, but are of the opposite sign, to the projected future changes in the no-SAI simulations (Figure 5 and 7). Further, the differences between the SAI and no-SAI simulations for MUCAPE, MUCIN and CAPES06 are widely statistically significant across the eastern U.S. for 2060-2069, while the differences for S06 are not (Figure 7).

In addition to examining changes in each convective weather environment parameter separately, understanding their co-variability can provide insight into the potential change in the distributions of convective modes and frequency with and without SAI (Diffenbaugh et al., 2013; Lepore et al., 2021; K. L. Rasmussen et al., 2017). To this point, bivariate distributions of convective weather environment parameters from 2060-2069 were created from daily data for the SAI and no-SAI simulations, respectively. For each individual ensemble member, daily mean values of MUCAPE, MUCIN and S06 were collected for each gridpoint over the Southeast in MAM and the Midwest in JJA.

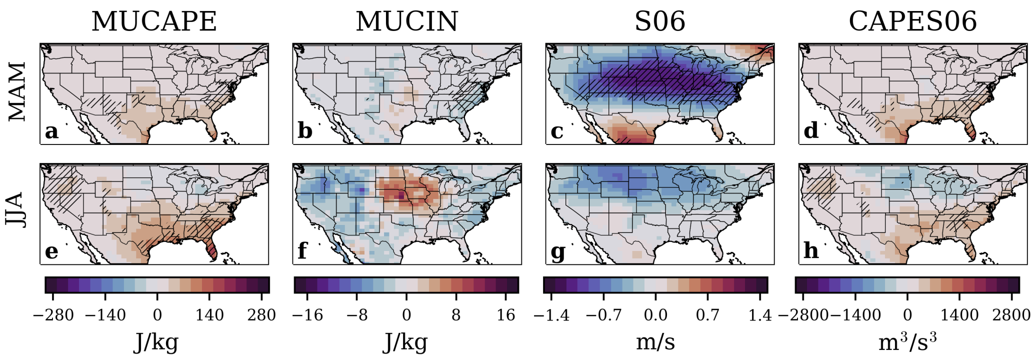

Figure 6: Differences between 2060-2069 (SAI) and 2015-2034 (SSP2-4.5) ensemble mean MUCAPE, MUCIN, S06, and CAPES06, in MAM (top row) and JJA (bottom row). Stippling indicates statistical significance at the α=0.05 level.

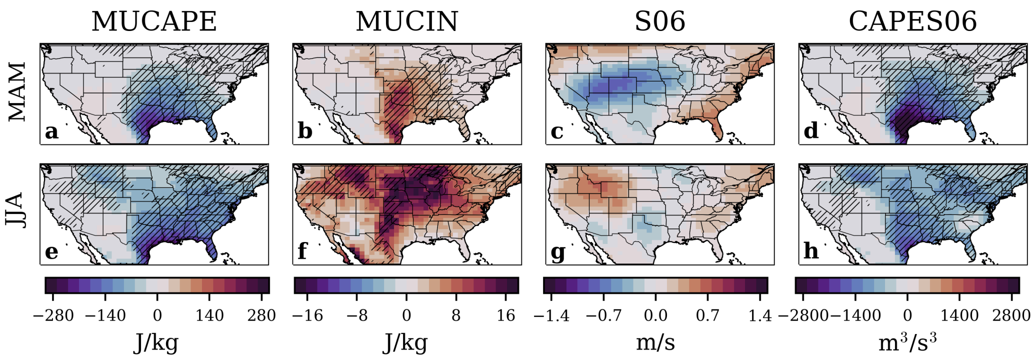

Figure 7: Differences between SAI and SSP2-4.5 ensemble means for 2060-2069 in MAM (top row) and JJA (bottom row). Stippling indicates statistical significance at the α=0.05 level.

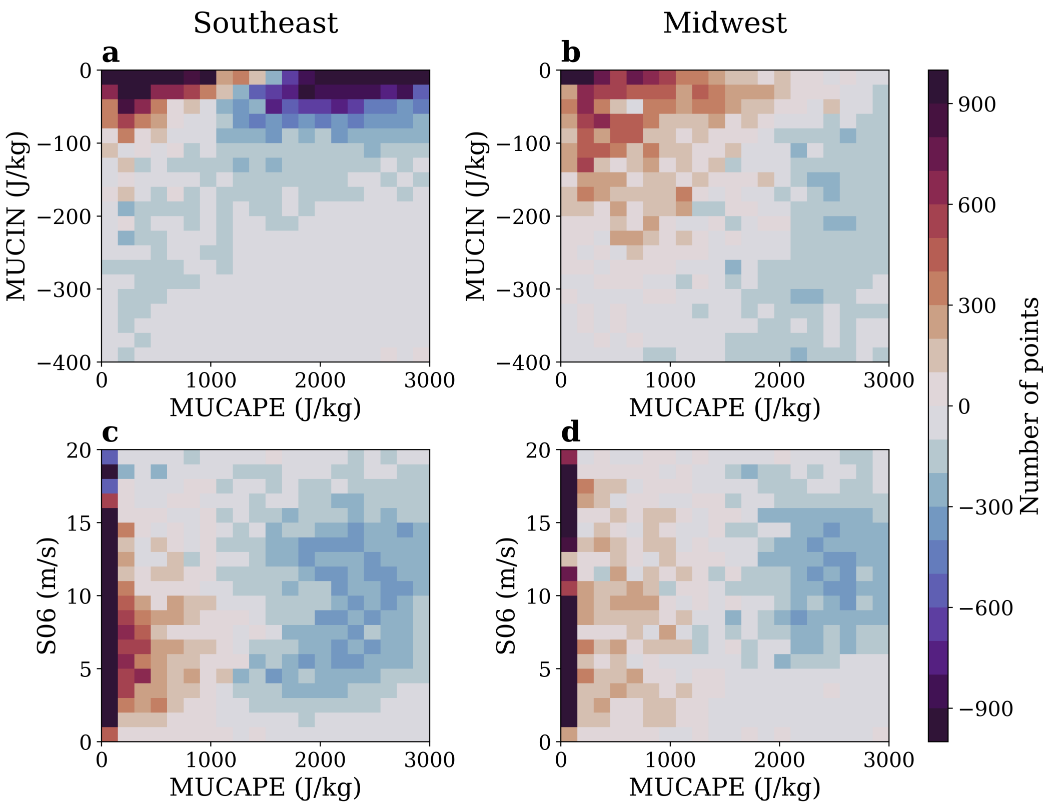

Figure 8: The difference between the SAI and no-SAI simulations (i.e., SAI - SSP2-4.5) for the bivariate distribution of MUCAPE (x-axis) and MUCIN (y-axis) for the Southeast in MAM (a) and the Midwest in JJA (b) over 2060-2069. (c) shows the difference between the SAI and no-SAI simulations for the bivariate distribution of MUCAPE (x-axis) and S06 (y-axis) for the Southeast in MAM, while (d) shows the same, but for the Midwest in JJA. Red (blue) pixels represent bins where there are more (less) days with corresponding MUCAPE and MUCIN (MUCAPE and S06) values in the simulations with SAI.

Distinct bivariate distributions (MUCAPE versus MUCIN, and MUCAPE versus S06) were then plotted for the difference of the SAI and no-SAI simulations (Figure 8). Positive numbers indicate that the SAI simulations had more days in a given bin than the no-SAI simulations, whereas negative numbers indicate the opposite.

In the Southeast in MAM and the Midwest in JJA, there are more days with low magnitudes of MUCAPE and MUCIN in the SAI simulations than in the no-SAI simulations, indicating that projected increases in the number of days with increased MUCAPE and MUCIN magnitudes under SSP2-4.5 could be largely avoided with SAI

(Figure 8a, 8b). The shift in the distribution of these parameters is due to decreases in both MUCAPE and MUCIN, which is evident in the straight diagonal region that separates the red and blue points. The difference in the shape of the distributions between the Southeast in MAM (Figure 8a) and the Midwest in JJA (Figure 8b) is largely due to the climatology of MUCIN, where values have much higher magnitudes in the Midwest in JJA (Figure 4b, 4f).

The difference between the SAI and no-SAI simulations for the daily bivariate distribution of MUCAPE and S06 is illustrated in Figure 8c and 8d. While the simulations suggest fewer days with high MUCAPE if SAI were to be deployed, the number of days with high shear is comparable between the SAI and no-SAI simulations. Thus, with SAI, there may be fewer days with high magnitude MUCAPE and S06, but the number of days with low-to-moderate MUCAPE and high shear may be similar with and without SAI (Figure 8c, 8d).

The analyses in Figure 8 also begin to highlight the potential role of unforced, internal climate variability in projected future changes in convective weather environments with and without SAI. The potential for internal variability to significantly modulate projected forced changes in climate is known to be significant (e.g. Deser et al., 2012; Deser, 2020; Schwarzwald and Lenssen, 2022). Motivated by these and similar studies, the next section goes beyond descriptions of only forced changes in climate warming in order to more completely examine the range of plausible future convective weather environments with and without SAI.

3.2 The Role of Internal Climate Variability

Other studies have examined the impact of internal climate variability on the behavior of severe weather related phenomena. However, they have tended to focus on sub-seasonal-to-interannual variations, such as those associated with the Madden Julian Oscillation (Baggett et al., 2018; Thompson & Roundy, 2013) or the El Niño Southern Oscillation (ENSO) phenomenon. For instance, J. T. Allen et al. (2018) examined the role of ENSO in modulating the annual cycle of tornadoes over the U.S., while Tippett et al. (2022) studied how ENSO and the phase of the Arctic Oscillation (AO) impacted the predictability of the tornado environment index. What has not been often considered, however, is the potential role that lower frequency (e.g., decadal) internal climate variability could play in future projections of severe weather. Ensemble simulations from climate and Earth system models indicate that even though the forced response to increasing greenhouse gas concentrations shows warming across the U.S. and other land regions, decadal and longer-timescale internal climate variability has the potential to significantly enhance or dampen the forced response (Deser et al., 2012; Hawkins & Sutton, 2009; Kay et al., 2015). It is thus relevant to consider how internal climate variability may impact future projections of convective weather environments both with and without SAI.

Histograms of changes in MUCAPE and CAPES06 by 2060-2069 relative to the reference period (2015-2034) show that while the forced response (ensemble mean) increases in magnitude under SSP2-4.5, changes in individual no-SAI simulations could be notably smaller or larger due to unforced variations in climate (Figure 9; gray bars). Specifically, individual ensemble members project changes in MUCAPE that depart as much as 60 J kg^{-1} from the ensemble mean increase of 107 J kg^{-1} by 2060-2069 over the Southeast in MAM (Figure 9a). Similar results are evident for CAPES06. For instance, while the ensemble-mean projected change in CAPES06 is an increase of 392 m^3 s^{-3} across the Midwest in JJA, one member projects a decrease of 226 m^3 s^{-3} by mid-century (Figure 9h). Such results confirm the large role that internal climate variability will likely play in the future evolution of climate, a point also emphasized recently by Franke et al. (2023) who examined future decadal trends in convective environment variables using the CESM2 Large Ensemble under SSP3-7.0 (Rodgers et al., 2021).

A similarly wide range of possible changes in MUCAPE, MUCIN and CAPES06 are also evident in the SAI simulations (Figure 9; red hatched bars). Thus, while the forced signals in the convective weather environment parameters examined here are distinct in future worlds with and without SAI, internal climate variability could produce similar climate outcomes in the decades ahead (Keys et al., 2022). For example, an ensemble member in the no-SAI simulation projects that MUCIN decreases in magnitude by 5.2 J kg^{-1} in the Midwest in JJA by 2060-2069, while a member in the SAI simulation projects an 8.5 J kg^{-1} increase in MUCIN over the same period (Figure 9f). Additionally, the distribution of possible future changes in S06 with and without SAI are very similar across ARISE-SAI ensemble members when averaged over the Southeast and Midwest regions, as is the case for the ensemble-mean changes (Figure 9c, 9g). This further

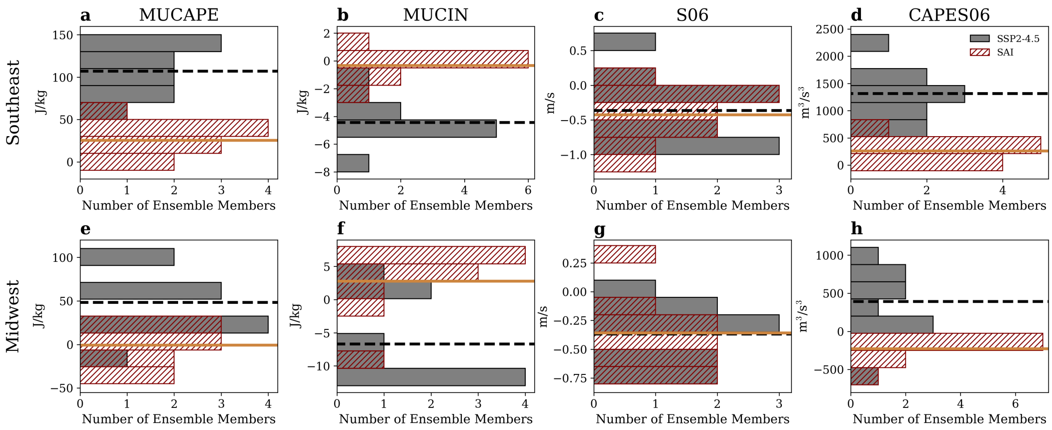

Figure 9: Histograms of the 10 ensemble members of the SSP2-4.5 (gray bars) and SAI (red hatched bars) simulations, illustrating the change in MUCAPE, MUCIN, S06, and CAPES06 for 2060-2069 relative to the 2015-2034. The black dotted and solid tan lines represent the ensemble mean values of the SSP2-4.5 and SAI simulations, respectively. Results are for the Southeast in MAM (a-d) and the Midwest in JJA (f-h).

supports the idea that the thermal wind relationship may not be the primary mechanism governing future changes in the deep-layer tropospheric wind shear over the U.S.

To further illustrate the extent to which internal climate variability can produce a climate outcome that differs significantly from the forced response alone, the ensemble member with the maximum change in CAPES06 by 2060-2069 when averaged over the Southeast in MAM is contrasted against the ensemble member with the smallest change. The spatial patterns of change for each of these two ensemble members is shown in Figure 10, along with the ensemble mean changes. By subtracting the latter from the total changes in CAPES06, the regional changes due only to internal climate variability are revealed. The main point is that internal climate variability may either significantly enhance the forced response due to climate change (Figure 10c) or suppress it (Figure 10f) on decadal time scales. It is also notable that the magnitudes of the changes due solely to internal climate variability are spatially coherent over large regions, and they are of similar magnitude to the force changes (e.g., Deser et al., 2020).

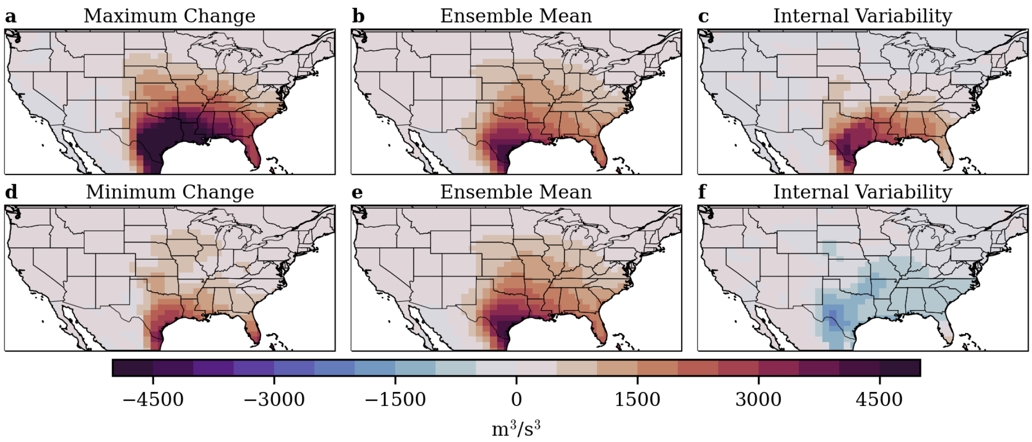

Figure 10: The ensemble members with the maximum (a) and minimum (b) changes in CAPES06 by 2060-2069 relative to 2015-2034 over the Southeast in MAM in the SSP2-4.5 simulations, calculation described in text. The forced response, or ensemble mean, is shown in (b) and repeated in (e). The change in CAPES06 due only to internal variability is shown for the ensemble member with the maximum and minimum change in (c) and (f), respectively.

4 Discussion

In ARISE-SAI, projected future changes in MUCAPE, MUCIN, and CAPES06 are smaller with simulated SAI deployment than what is projected with climate change alone (Figure 5, 6). This is consistent with lower temperatures and dew points on average throughout the troposphere in MAM and JJA in an SAI future (Figure S2). It thus follows that the SAI simulations have fewer co-occurrences of high magnitude MUCAPE and MUCIN in the future (Figure 8a, 8b), whereas changes in the bivariate distribution of MUCAPE and S06 are primarily driven by smaller values of MUCAPE in a future with SAI (Figure 8c, 8d).

Future differences in tropospheric wind shear are more difficult to understand than SAI-induced changes in thermodynamic parameters. Under climate change with and without SAI, S06 is expected to decrease across much of the convectively active regions in the U.S. in the spring and summer seasons (Figure 5c, 5g, 6c, 6g). Although the decreases are small in magnitude relative to the climatology (Figure 4c, 4g), similar decreases have been documented in other studies of future climate change. Trapp et al. (2007), for instance, concluded that future decreases in tropospheric wind shear are consistent with decreases in the middle latitude thermal wind, as would be expected as the equator-to-pole temperature gradient decreases over the 21st century (Cohen et al., 2014; Francis & Vavrus, 2012). However, changes in S06 with SAI are broadly consistent with those in the no-SAI simulations examined here (Figure 5c, 5g, 6c, 6g), even though ARISE-SAI is configured so that the equator-to-pole temperature gradient remains near its 2035 value when SAI is deployed (Richter et al., 2022).

While a detailed analysis of the changes in wind shear are beyond the scope of this study, note that precipitation is projected to increase over the eastern equatorial Pacific during the seasons examined here under both the SAI and no-SAI simulations, although the increases projected with SAI are smaller in magnitude (Figure S3; see also Richter et al., 2022). Simpson et al. (2019) also indicated that precipitation is projected to increase in magnitude in the eastern equatorial Pacific in a future with SAI. Further, they examined the precipitation response to the addition of stratospheric heating in the absence of a greenhouse gas forcing, and found that precipitation is also projected to increase in the eastern equatorial Pacific. This suggests that precipitation changes in this region are influenced by dynamical responses that may result from the introduction of aerosols into the stratosphere. Upper-level divergence due to tropical convective heating in the equatorial Pacific can be the source of anomalous vorticity that drives the propagation of Rossby wave trains that impact the extratropics (Qin & Robinson, 1993; Sardeshmukh & Hoskins, 1988). This idea is broadly consistent with the spatial patterns of 300 hPa winds in both the SAI and no-SAI simulations, with alternating bands of increasing and decreasing winds emanating from the eastern tropical Pacific (Figure S4). In other words, future changes in S06 in the SAI and no-SAI simulations may be driven by changes in tropical precipitation and associated large-scale climate circulations, which are similar whether or not SAI is deployed.

A novel aspect of this study is the use of individual ensemble members to examine the variability around the forced responses to climate change and SAI in large-scale convective weather environment parameters relevant to severe weather (Figure 9). Recall that each individual ensemble member represents an equally-plausible climate outcome in the decades ahead (e.g., Deser et al., 2020). The results illustrate the large-role internal climate variability will likely have, especially on regional scales. This also means that future convective weather environments in an SAI world could be indistinguishable from a world without SAI, even though the forced responses are distinguishable. Note that a 10-member ensemble is likely insufficient to statistically capture the full breadth of possible outcomes (Deser et al., 2012; Franke et al., 2023). There are also shortcomings in the ability of Earth-system models to accurately represent internal climate variability (Orbe et al., 2020; O'Reilly et al., 2021).

Other limitations of this study include the fact that the use of large-scale parameters to assess how the behavior of severe weather may change in the future is itself a caveat, since a favorable environment does not imply that convection will actually occur. Further, this method assumes that the frequency of convective initiation will not change with climate warming (Hoogewind et al., 2017; Trapp et al., 2007, 2009), and that the rate of initiation would not be affected by SAI deployment. Convective initiation is dependent on a variety of factors such as orography and large-scale dynamics, the latter of which have the potential to be impacted by climate warming and potential SAI deployment. The representation of convective initiation is also likely sensitive to model configuration (Carlson et al., 1983; Trapp et al., 2007).

5 Conclusion

The potential impact of SAI on future convective weather environments across the U.S. Midwest and Southeast was evaluated in one climate change scenario, with and without SAI deployment. The ARISE-SAI simulations indicate that, with climate change, thermodynamic parameters such as MUCAPE and MUCIN are projected to increase in magnitude across the U.S. in the spring and summer, and that these increases could be mostly avoided if SAI were to be deployed. Future changes in kinematic parameters, such as S06, appear to be primarily driven by changes in precipitation over the eastern tropical Pacific, which are similar between climate change simulations with and without SAI. Results further indicate that internal climate variability has the potential to significantly impact future projections of U.S. convective weather environments regionally, with spatially-coherent changes of similar magnitude to the forced responses.

Future work could examine how model-specific biases impact future projections of convective weather environments with and without SAI. For instance, the exact ARISE-SAI scenarios examined here were recently completed using the first version of the U.K. Earth System Model (Archibald et al., 2020; Sellar et al., 2019; Henry et al., 2023).

It would also be insightful to examine Earth-system model simulations with different SAI deployment goals and timelines (e.g., MacMartin et al., 2022), as well as simulations under different climate change scenarios, such as the Stratospheric Aerosol Geoengineering Large Ensemble Project (Tilmes et al., 2018). Use of the output from Earth-system models to force high-resolution, regional climate models to explicitly examine how projected changes in the large-scale environment impact the distribution of convective modes could provide additional understanding as to how SAI deployment impacts convective weather (Ashley et al., 2023; Gensini et al., 2023; Gensini & Mote, 2015; K. L. Rasmussen et al., 2017; Trapp et al., 2019).

6 Open Research

The original ARISE-SAI data set from which the data in this work was derived (all SAI members and 5 no-SAI members) are located on the NCAR Climate Data Gateway (Richter, 2022a, https://doi.org/10.5065/9kcn-9y79). The remaining 5 no-SAI members are available from the NCAR Climate Data Gateway at (Richter, 2022b, https://doi.org/10.26024/0cs0-ev98). All ARISE-SAI data may also be accessed from Amazon Web Services (NCAR, 2022, registry.opendata.aws/ncar-cesm2-arise/). The complete CESM2 (WACCM6) Historical runs from which the data in this work was derived are available at Earth System Grid (Danabasoglu, 2019, https://doi.org/10.22033/ESGF/CMIP6.11298).

Acknowledgments

This work was supported by the National Oceanic and Atmospheric Administration (NOAA grant #NA22OAR4320473) and the LAD Climate Group. The ARISE-SAI simulations were produced by the National Center for Atmospheric Research (NCAR) with support from the National Science Foundation (NSF; grant no. 1852977) and by SilverLining through its Safe Climate Research Initiative. The CESM2 (WACCM6) Historical simulations were produced by NCAR. The CESM project is supported primarily by NSF.

References

Abiodun, B. J., Odoulami, R. C., Sawadogo, W., Oloniyo, O. A., Abatan, A. A., New, M., … MacMartin, D. G. (2021, December). Potential impacts of stratospheric aerosol injection on drought risk managements over major river basins in Africa. *Climatic Change*, *169*(3), 31. Retrieved 2023-02-13, from https://doi.org/10.1007/s10584-021-03268-w doi: 10.1007/s10584-021-03268-w

Allen, J. T., Molina, M. J., & Gensini, V. A. (2018). Modulation of Annual Cycle of Tornadoes by El Niño–Southern Oscillation. *Geophysical Research Letters*, *45*(11), 5708–5717. Retrieved 2023-03-30, from https://onlinelibrary.wiley.com/doi/abs/10.1029/2018GL077482 (_eprint: https://onlinelibrary.wiley.com/doi/pdf/10.1029/2018GL077482) doi: 10.1029/2018GL077482

Allen, M. R., & Ingram, W. J. (2002, September). Constraints on future changes in climate and the hydrologic cycle. *Nature*, *419*(6903), 224–232. Retrieved 2023-01-20, from https://www.nature.com/articles/nature01092 (Number: 6903 Publisher: Nature Publishing Group) doi: 10.1038/nature01092

Archibald, A. T., O'Connor, F. M., Abraham, N. L., Archer-Nicholls, S., Chipperfield, M. P., Dalvi, M., ... Zeng, G. (2020, March). Description and evaluation of the UKCA stratosphere–troposphere chemistry scheme (StratTrop vn 1.0) implemented in UKESM1. *Geoscientific Model Development*, *13*(3), 1223–1266. Retrieved 2023-03-24, from https://gmd.copernicus.org/articles/13/1223/2020/ (Publisher: Copernicus GmbH) doi: 10.5194/gmd-13-1223-2020

Ashley, W. S., Haberlie, A. M., & Gensini, V. A. (2023, January). The Future of Supercells in the United States. *Bulletin of the American Meteorological Society*, *104*(1), E1–E21. Retrieved 2023-01-17, from https://journals.ametsoc.org/view/journals/bams/104/1/BAMS-D-22-0027.1.xml doi: 10.1175/BAMS-D-22-0027.1

Baggett, C. F., Nardi, K. M., Childs, S. J., Zito, S. N., Barnes, E. A., & Maloney, E. D. (2018). Skillful Subseasonal Forecasts of Weekly Tornado and Hail Activity Using the Madden-Julian Oscillation. *Journal of Geophysical Research: Atmospheres*, *123*(22), 12,661–12,675. Retrieved 2023-05-22, from https://onlinelibrary.wiley.com/doi/abs/10.1029/2018JD029059 (_eprint: https://onlinelibrary.wiley.com/doi/pdf/10.1029/2018JD029059) doi: 10.1029/2018JD029059

Barnes, E. A., Hurrell, J. W., & Sun, L. (2022). Detecting Changes in Global Extremes

Under the GLENS-SAI Climate Intervention Strategy. *Geophysical Research Letters*, *49*(20), e2022GL100198. Retrieved 2022-11-08, from `https://onlinelibrary.wiley.com/doi/abs/10.1029/2022GL100198` (_eprint: https://onlinelibrary.wiley.com/doi/pdf/10.1029/2022GL100198) doi: 10.1029/2022GL100198

Bednarz, E. M., Visioni, D., Richter, J. H., Butler, A. H., & MacMartin, D. G. (2022). Impact of the Latitude of Stratospheric Aerosol Injection on the Southern Annular Mode. *Geophysical Research Letters*, *49*(19), e2022GL100353. Retrieved 2023-05-23, from `https://onlinelibrary.wiley.com/doi/abs/10.1029/2022GL100353` (_eprint: https://onlinelibrary.wiley.com/doi/pdf/10.1029/2022GL100353) doi: 10.1029/2022GL100353

Brooks, H. E., Anderson, A. R., Riemann, K., Ebbers, I., & Flachs, H. (2007, February). Climatological aspects of convective parameters from the NCAR/NCEP reanalysis. *Atmospheric Research*, *83*(2), 294–305. Retrieved 2022-08-04, from `https://www.sciencedirect.com/science/article/pii/S0169809506001128` doi: 10.1016/j.atmosres.2005.08.005

Brooks, H. E., Doswell, C. A., & Kay, M. P. (2003, August). Climatological Estimates of Local Daily Tornado Probability for the United States. *Weather and Forecasting*, *18*(4), 626–640. Retrieved 2023-01-17, from `https://journals.ametsoc.org/view/journals/wefo/18/4/1520-0434_2003_018_0626_ceoldt_2_0_co_2.xml` (Publisher: American Meteorological Society Section: Weather and Forecasting) doi: 10.1175/1520-0434(2003)018⟨0626:CEOLDT⟩2.0.CO;2

Carlson, T. N., Benjamin, S. G., Forbes, G. S., & Li, Y.-F. (1983, July). Elevated Mixed Layers in the Regional Severe Storm Environment: Conceptual Model and Case Studies. *Monthly Weather Review*, *111*(7), 1453–1474. Retrieved 2023-04-04, from `https://journals.ametsoc.org/view/journals/mwre/111/7/1520-0493_1983_111_1453_emlitr_2_0_co_2.xml` (Publisher: American Meteorological Society Section: Monthly Weather Review) doi: 10.1175/1520-0493(1983)111⟨1453:EMLITR⟩2.0.CO;2

Chen, J., Dai, A., Zhang, Y., & Rasmussen, K. L. (2020, February). Changes in Convective Available Potential Energy and Convective Inhibition under Global Warming. *Journal of Climate*, *33*(6), 2025–2050. Retrieved 2023-05-18, from `https://journals.ametsoc.org/view/journals/clim/33/6/`

jcli-d-19-0461.1.xml (Publisher: American Meteorological Society Section: Journal of Climate) doi: 10.1175/JCLI-D-19-0461.1

Cohen, J., Screen, J. A., Furtado, J. C., Barlow, M., Whittleston, D., Coumou, D., ... Jones, J. (2014, September). Recent Arctic amplification and extreme mid-latitude weather. *Nature Geoscience*, *7*(9), 627–637. Retrieved 2023-05-01, from https://www.nature.com/articles/ngeo2234 (Number: 9 Publisher: Nature Publishing Group) doi: 10.1038/ngeo2234

Craven, J. P., & Brooks, H. E. (2004). BASELINE CLIMATOLOGY OF SOUNDING DERIVED PARAMETERS ASSOCIATED WITH DEEP MOIST CONVECTION. *National Weather Digest*, *28*.

Crutzen, P. J. (2006, August). Albedo Enhancement by Stratospheric Sulfur Injections: A Contribution to Resolve a Policy Dilemma? *Climatic Change*, *77*(3-4), 211. Retrieved 2022-06-08, from https://link.springer.com/10.1007/s10584-006-9101-y doi: 10.1007/s10584-006-9101-y

Danabasoglu, G. (2019). *NCAR CESM2-WACCM-FV2 model output prepared for CMIP6 CMIP historical.* Earth System Grid Federation. Retrieved 2023-07-14, from https://doi.org/10.22033/ESGF/CMIP6.11298 doi: 10.22033/ESGF/CMIP6.11298

Danabasoglu, G., Lamarque, J.-F., Bacmeister, J., Bailey, D. A., DuVivier, A. K., Edwards, J., ... Strand, W. G. (2020). The Community Earth System Model Version 2 (CESM2). *Journal of Advances in Modeling Earth Systems*, *12*(2), e2019MS001916. Retrieved 2022-12-01, from https://onlinelibrary.wiley.com/doi/abs/10.1029/2019MS001916 (_eprint: https://onlinelibrary.wiley.com/doi/pdf/10.1029/2019MS001916) doi: 10.1029/2019MS001916

Deser, C., Knutti, R., Solomon, S., & Phillips, A. S. (2012, November). Communication of the role of natural variability in future North American climate. *Nature Climate Change*, *2*(11), 775–779. Retrieved 2023-03-21, from https://www.nature.com/articles/nclimate1562 (Number: 11 Publisher: Nature Publishing Group) doi: 10.1038/nclimate1562

Deser, C., Lehner, F., Rodgers, K. B., Ault, T., Delworth, T. L., DiNezio, P. N., ... Ting, M. (2020, April). Insights from Earth system model initial-condition large ensembles and future prospects. *Nature Climate Change*, *10*(4), 277–286. Retrieved 2023-01-23, from https://www.nature.com/articles/s41558-020-0731-2 (Number: 4 Publisher: Nature Publishing Group) doi: 10.1038/s41558-020-0731-2

Diffenbaugh, N. S., Scherer, M., & Trapp, R. J. (2013, October). Robust increases in severe thunderstorm environments in response to greenhouse forcing. *Proceedings of the National Academy of Sciences*, *110*(41), 16361–16366. Retrieved 2023-01-17, from https://www.pnas.org/doi/10.1073/pnas.1307758110 (Publisher: Proceedings of the National Academy of Sciences) doi: 10.1073/pnas.1307758110

Donat, M. G., Lowry, A. L., Alexander, L. V., O'Gorman, P. A., & Maher, N. (2016, May). More extreme precipitation in the world's dry and wet regions. *Nature Climate Change*, *6*(5), 508–513. Retrieved 2023-01-20, from https://www.nature.com/articles/nclimate2941 (Number: 5 Publisher: Nature Publishing Group) doi: 10.1038/nclimate2941

Doswell, C. A., Brooks, H. E., & Kay, M. P. (2005, August). Climatological Estimates of Daily Local Nontornadic Severe Thunderstorm Probability for the United States. *Weather and Forecasting*, *20*(4), 577–595. Retrieved 2022-08-08, from https://journals.ametsoc.org/view/journals/wefo/20/4/waf866_1.xml (Publisher: American Meteorological Society Section: Weather and Forecasting) doi: 10.1175/WAF866.1

Doswell, C. A., Brooks, H. E., & Maddox, R. A. (1996, December). Flash Flood Forecasting: An Ingredients-Based Methodology. *Weather and Forecasting*, *11*(4), 560–581. Retrieved 2022-08-08, from https://journals.ametsoc.org/view/journals/wefo/11/4/1520-0434_1996_011_0560_fffaib_2_0_co_2.xml (Publisher: American Meteorological Society Section: Weather and Forecasting) doi: 10.1175/1520-0434(1996)011⟨0560:FFFAIB⟩2.0.CO;2

Doswell, C. A., & Rasmussen, E. N. (1994, December). The Effect of Neglecting the Virtual Temperature Correction on CAPE Calculations. *Weather and Forecasting*, *9*(4), 625–629. Retrieved 2023-01-18, from https://journals.ametsoc.org/view/journals/wefo/9/4/1520-0434_1994_009_0625_teontv_2_0_co_2.xml (Publisher: American Meteorological Society Section: Weather and Forecasting) doi: 10.1175/1520-0434(1994)009⟨0625:TEONTV⟩2.0.CO;2

Dougherty, E., & Rasmussen, K. L. (2020, October). Changes in Future Flash Flood–Producing Storms in the United States. *Journal of Hydrometeorology*, *21*(10), 2221–2236. Retrieved 2023-08-02, from https://journals.ametsoc.org/view/journals/hydr/21/10/jhmD200014.xml (Publisher: American Meteorological Society Section: Journal of Hydrometeorology) doi: 10.1175/JHM-D-20-0014.1

Eyring, V., Bony, S., Meehl, G. A., Senior, C. A., Stevens, B., Stouffer, R. J., & Taylor, K. E. (2016, May). Overview of the Coupled Model Intercomparison Project Phase 6 (CMIP6) experimental design and organization. *Geoscientific Model Development*, *9*(5), 1937–1958. Retrieved 2023-04-03, from https://gmd.copernicus.org/articles/9/1937/2016/ (Publisher: Copernicus GmbH) doi: 10.5194/gmd-9-1937-2016

Francis, J. A., & Vavrus, S. J. (2012). Evidence linking Arctic amplification to extreme weather in mid-latitudes. *Geophysical Research Letters*, *39*(6). Retrieved 2023-05-01, from https://onlinelibrary.wiley.com/doi/abs/10.1029/2012GL051000 (_eprint: https://onlinelibrary.wiley.com/doi/pdf/10.1029/2012GL051000) doi: 10.1029/2012GL051000

Franke, M. E., Hurrell, J. W., Rasmussen, K., & Sun, L. (2023, January). *Impacts of Forced and Internal Climate Variability on Changes in Convective Environments Over the Eastern United States* (preprint). Preprints. Retrieved 2023-05-04, from https://essopenarchive.org/users/578629/articles/620460-impacts-of-forced-and-internal-climate-variability-on-changes-in-convective-environments-over-the-eastern-united-states?commit=f280406d36d6436beeabb633ec5ae9f65dca7b99 doi: 10.22541/essoar.167458066.68764316/v1

Friedlingstein, P., O'Sullivan, M., Jones, M. W., Andrew, R. M., Gregor, L., Hauck, J., … Zheng, B. (2022, November). Global Carbon Budget 2022. *Earth System Science Data*, *14*(11), 4811–4900. Retrieved 2023-02-08, from https://essd.copernicus.org/articles/14/4811/2022/ (Publisher: Copernicus GmbH) doi: 10.5194/essd-14-4811-2022

Galway, J. G. (1989, December). The Evolution of Severe Thunderstorm Criteria within the Weather Service. *Weather and Forecasting*, *4*(4), 585–592. Retrieved 2023-05-23, from https://journals.ametsoc.org/view/journals/wefo/4/4/1520-0434_1989_004_0585_teostc_2_0_co_2.xml (Publisher: American

Meteorological Society Section: Weather and Forecasting) doi: 10.1175/1520-0434(1989)004⟨0585:TEOSTC⟩2.0.CO;2

Gensini, V. A., Haberlie, A. M., & Ashley, W. S. (2023, January). Convection-permitting simulations of historical and possible future climate over the contiguous United States. *Climate Dynamics*, *60*(1), 109–126. Retrieved 2023-01-17, from https://doi.org/10.1007/s00382-022-06306-0 doi: 10.1007/s00382-022-06306-0

Gensini, V. A., & Mote, T. L. (2015, March). Downscaled estimates of late 21st century severe weather from CCSM3. *Climatic Change*, *129*(1), 307–321. Retrieved 2022-11-29, from https://doi.org/10.1007/s10584-014-1320-z doi: 10.1007/s10584-014-1320-z

Gettelman, A., Mills, M. J., Kinnison, D. E., Garcia, R. R., Smith, A. K., Marsh, D. R., . . . Randel, W. J. (2019). The Whole Atmosphere Community Climate Model Version 6 (WACCM6). *Journal of Geophysical Research: Atmospheres*, *124*(23), 12380–12403. Retrieved 2023-01-17, from https://onlinelibrary.wiley.com/doi/abs/10.1029/2019JD030943 (_eprint: https://onlinelibrary.wiley.com/doi/pdf/10.1029/2019JD030943) doi: 10.1029/2019JD030943

Hawkins, E., & Sutton, R. (2009, August). The Potential to Narrow Uncertainty in Regional Climate Predictions. *Bulletin of the American Meteorological Society*, *90*(8), 1095–1108. Retrieved 2023-04-03, from https://journals.ametsoc.org/view/journals/bams/90/8/2009bams2607_1.xml (Publisher: American Meteorological Society Section: Bulletin of the American Meteorological Society) doi: 10.1175/2009BAMS2607.1

Henry, M., Haywood, J., Jones, A., Dalvi, M., Wells, A., Visioni, D., . . . Tye, M. (2023, June). Comparison of UKESM1 and CESM2 Simulations Using the Same Multi-Target Stratospheric Aerosol Injection Strategy. *EGUsphere*, 1–22. Retrieved 2023-08-07, from https://egusphere.copernicus.org/preprints/2023/egusphere-2023-980/ (Publisher: Copernicus GmbH) doi: 10.5194/egusphere-2023-980

Hoogewind, K. A., Baldwin, M. E., & Trapp, R. J. (2017, December). The Impact of Climate Change on Hazardous Convective Weather in the United States: Insight from High-Resolution Dynamical Downscaling. *Journal of Climate*, *30*(24), 10081–10100. Retrieved 2023-01-24, from https://journals.ametsoc.org/view/journals/clim/30/24/jcli-d-16-0885.1.xml (Publisher: American Meteorological Society Section: Journal of Climate) doi: 10.1175/JCLI-D-16-0885.1

Hueholt, D. M., Barnes, E. A., Hurrell, J. W., Richter, J. H., & Sun, L. (2023, February). *Assessing Outcomes in Stratospheric Aerosol Injection Scenarios Shortly After Deployment* (preprint). Preprints. Retrieved 2023-05-04, from https://essopenarchive.org/users/580207/articles/621364-assessing-outcomes-in-stratospheric-aerosol-injection-scenarios-shortly-after-deployment?commit=cd38f22b1228a1414f057f4cb5c866be8991006f doi: 10.22541/essoar.167591089.94758275/v1

IPCC. (2021). Summary for Policymakers.

Ji, D., Fang, S., Curry, C. L., Kashimura, H., Watanabe, S., Cole, J. N. S., ... Moore, J. C. (2018, July). Extreme temperature and precipitation response to solar dimming and stratospheric aerosol geoengineering. *Atmospheric Chemistry and Physics*, *18*(14), 10133–10156. Retrieved 2023-04-19, from https://acp.copernicus.org/articles/18/10133/2018/ (Publisher: Copernicus GmbH) doi: 10.5194/acp-18-10133-2018

Jiang, X., & Guan, D. (2016). Determinants of global CO2 emissions growth. *Applied Energy*, *184*(C), 1132–1141. Retrieved 2023-05-23, from https://econpapers.repec.org/article/eeeappene/v_3a184_3ay_3a2016_3ai_3ac_3ap_3a1132-1141.htm (Publisher: Elsevier)

Kay, J. E., Deser, C., Phillips, A., Mai, A., Hannay, C., Strand, G., ... Vertenstein, M. (2015, August). The Community Earth System Model (CESM) Large Ensemble Project: A Community Resource for Studying Climate Change in the Presence of Internal Climate Variability. *Bulletin of the American Meteorological Society*, *96*(8), 1333–1349. Retrieved 2022-05-12, from https://journals.ametsoc.org/view/journals/bams/96/8/bams-d-13-00255.1.xml (Publisher: American Meteorological Society Section: Bulletin of the American Meteorological Society) doi: 10.1175/BAMS-D-13-00255.1

Kelly, D. L., Schaefer, J. T., & Doswell, C. A. (1985, November). Climatology of Nontornadic Severe Thunderstorm Events in the United States. *Monthly Weather Review*, *113*(11), 1997–2014. Retrieved 2022-08-08, from https://journals.ametsoc.org/view/journals/mwre/113/11/1520-0493_1985_113_1997_conste_2_0_co_2.xml (Publisher: American Meteorological Society Section: Monthly Weather Review) doi: 10.1175/1520-0493(1985)113⟨1997:CONSTE⟩2.0.CO;2

Keys, P. W., Barnes, E. A., Diffenbaugh, N. S., Hurrell, J. W., & Bell, C. M. (2022, October). Potential for perceived failure of stratospheric aerosol injection deployment. *Proceedings of the National Academy of Sciences*, *119*(40), e2210036119. Retrieved 2022-11-09, from https://www.pnas.org/doi/full/10.1073/pnas.2210036119 (Publisher: Proceedings of the National Academy of Sciences) doi: 10.1073/pnas.2210036119

Kravitz, B., MacMartin, D. G., Mills, M. J., Richter, J. H., Tilmes, S., Lamarque, J.-F., ... Vitt, F. (2017). First Simulations of Designing Stratospheric Sulfate Aerosol Geoengineering to Meet Multiple Simultaneous Climate Objectives. *Journal of Geophysical Research: Atmospheres*, *122*(23), 12,616–12,634. Retrieved 2023-04-20, from https://onlinelibrary.wiley.com/doi/abs/10.1002/2017JD026874 (_eprint: https://onlinelibrary.wiley.com/doi/pdf/10.1002/2017JD026874) doi: 10.1002/2017JD026874

Kravitz, B., Robock, A., Boucher, O., Schmidt, H., Taylor, K. E., Stenchikov, G., & Schulz, M. (2011). The Geoengineering Model Intercomparison Project (GeoMIP). *Atmospheric Science Letters*, *12*(2), 162–167. Retrieved 2023-04-20, from https://onlinelibrary.wiley.com/doi/abs/10.1002/asl.316 (_eprint: https://onlinelibrary.wiley.com/doi/pdf/10.1002/asl.316) doi: 10.1002/asl.316

Lee, W. R., MacMartin, D. G., Visioni, D., Kravitz, B., Chen, Y., Moore, J. C., ... Bailey, D. A. (2023). High-Latitude Stratospheric Aerosol Injection to Preserve the Arctic. *Earth's Future*, *11*(1), e2022EF003052. Retrieved 2023-04-19, from https://onlinelibrary.wiley.com/doi/abs/10.1029/2022EF003052 (_eprint: https://onlinelibrary.wiley.com/doi/pdf/10.1029/2022EF003052) doi: 10.1029/2022EF003052

Lepore, C., Abernathey, R., Henderson, N., Allen, J. T., & Tippett, M. K. (2021). Future Global Convective Environments in CMIP6 Models. *Earth's Future*, *9*(12), e2021EF002277. Retrieved 2022-06-27, from https://onlinelibrary.wiley.com/doi/abs/10.1029/2021EF002277 (_eprint: https://onlinelibrary.wiley.com/doi/pdf/10.1029/2021EF002277) doi:

10.1029/2021EF002277

Li, F., Chavas, D. R., Reed, K. A., & Ii, D. T. D. (2020, October). Climatology of Severe Local Storm Environments and Synoptic-Scale Features over North America in ERA5 Reanalysis and CAM6 Simulation. *Journal of Climate*, *33*(19), 8339–8365. Retrieved 2023-04-25, from https://journals.ametsoc.org/view/journals/clim/33/19/jcliD190986.xml (Publisher: American Meteorological Society Section: Journal of Climate) doi: 10.1175/JCLI-D-19-0986.1

Lockley, A., Xu, Y., Tilmes, S., Sugiyama, M., Rothman, D., & Hindes, A. (2022, July). 18 Politically relevant solar geoengineering scenarios. *Socio-Environmental Systems Modelling*, *4*, 18127–18127. Retrieved 2022-08-10, from https://sesmo.org/article/view/18127 doi: 10.18174/sesmo.18127

MacMartin, D. G., Kravitz, B., Keith, D. W., & Jarvis, A. (2014, July). Dynamics of the coupled human–climate system resulting from closed-loop control of solar geoengineering. *Climate Dynamics*, *43*(1), 243–258. Retrieved 2023-04-20, from https://doi.org/10.1007/s00382-013-1822-9 doi: 10.1007/s00382-013-1822-9

MacMartin, D. G., Visioni, D., Kravitz, B., Richter, J., Felgenhauer, T., Lee, W. R., ... Sugiyama, M. (2022, August). Scenarios for modeling solar radiation modification. *Proceedings of the National Academy of Sciences*, *119*(33), e2202230119. Retrieved 2022-08-10, from https://www.pnas.org/doi/full/10.1073/pnas.2202230119 (Publisher: Proceedings of the National Academy of Sciences) doi: 10.1073/pnas.2202230119

Marsh, P. T., Brooks, H. E., & Karoly, D. J. (2007). Assessment of the severe weather environment in North America simulated by a global climate model. *Atmospheric Science Letters*, *8*(4), 100–106. Retrieved 2023-05-23, from https://onlinelibrary.wiley.com/doi/abs/10.1002/asl.159 (_eprint: https://rmets.onlinelibrary.wiley.com/doi/pdf/10.1002/asl.159) doi: 10.1002/asl.159

Moore, J. C., Yue, C., Zhao, L., Guo, X., Watanabe, S., & Ji, D. (2019). Greenland Ice Sheet Response to Stratospheric Aerosol Injection Geoengineering. *Earth's Future*, *7*(12), 1451–1463. Retrieved 2023-04-19, from https://onlinelibrary.wiley.com/doi/abs/10.1029/2019EF001393 (_eprint: https://onlinelibrary.wiley.com/doi/pdf/10.1029/2019EF001393) doi:

10.1029/2019EF001393

Mukherjee, S., Mishra, A., & Trenberth, K. E. (2018, June). Climate Change and Drought: a Perspective on Drought Indices. *Current Climate Change Reports*, *4*(2), 145–163. Retrieved 2023-01-20, from https://doi.org/10.1007/s40641-018-0098-x doi: 10.1007/s40641-018-0098-x

NASEM. (2021). *Reflecting Sunlight: Recommendations for Solar Geoengineering Research and Research Governance*. Washington, D.C.: National Academies Press. Retrieved 2023-01-25, from https://www.nap.edu/catalog/25762 doi: 10.17226/25762

NCAR. (2022). *Community Earth System Model v2 ARISE (CESM2 ARISE) - Registry of Open Data on AWS.* Retrieved 2023-07-14, from https://registry.opendata.aws/ncar-cesm2-arise/

NCEI, A. B. (2022). *U.S. Billion-dollar Weather and Climate Disasters, 1980 - present (NCEI Accession 0209268).* NOAA National Centers for Environmental Information. Retrieved 2023-01-20, from https://www.ncei.noaa.gov/archive/accession/0209268 doi: 10.25921/STKW-7W73

Orbe, C., Roekel, L. V., Adames, F., Dezfuli, A., Fasullo, J., Gleckler, P. J., ... Zhao, M. (2020, September). Representation of Modes of Variability in Six U.S. Climate Models. *Journal of Climate*, *33*(17), 7591–7617. Retrieved 2023-04-04, from https://journals.ametsoc.org/view/journals/clim/33/17/jcliD190956.xml (Publisher: American Meteorological Society Section: Journal of Climate) doi: 10.1175/JCLI-D-19-0956.1

O'Neill, B. C., Kriegler, E., Ebi, K. L., Kemp-Benedict, E., Riahi, K., Rothman, D. S., ... Solecki, W. (2017, January). The roads ahead: Narratives for shared socioeconomic pathways describing world futures in the 21st century. *Global Environmental Change*, *42*, 169–180. Retrieved 2023-04-03, from https://www.sciencedirect.com/science/article/pii/S0959378015000060 doi: 10.1016/j.gloenvcha.2015.01.004

O'Reilly, C. H., Befort, D. J., Weisheimer, A., Woollings, T., Ballinger, A., & Hegerl, G. (2021, September). Projections of northern hemisphere extratropical climate underestimate internal variability and associated uncertainty. *Communications Earth & Environment*, *2*(1), 1–9. Retrieved 2023-03-30, from https://www.nature.com/articles/s43247-021-00268-7 (Number: 1 Publisher: Nature Publishing Group) doi: 10.1038/s43247-021-00268-7

Peters, G. P., Marland, G., Le Quéré, C., Boden, T., Canadell, J. G., & Raupach, M. R. (2012, January). Rapid growth in CO2 emissions after the 2008–2009 global financial crisis. *Nature Climate Change*, *2*(1), 2–4. Retrieved 2023-05-23, from https://www.nature.com/articles/nclimate1332 (Number: 1 Publisher: Nature Publishing Group) doi: 10.1038/nclimate1332

Prein, A. F., Rasmussen, R. M., Ikeda, K., Liu, C., Clark, M. P., & Holland, G. J. (2017, January). The future intensification of hourly precipitation extremes. *Nature Climate Change*, *7*(1), 48–52. Retrieved 2023-08-02, from https://www.nature.com/articles/nclimate3168 (Number: 1 Publisher: Nature Publishing Group) doi: 10.1038/nclimate3168

Qin, J., & Robinson, W. A. (1993, June). On the Rossby Wave Source and the Steady Linear Response to Tropical Forcing. *Journal of the Atmospheric Sciences*, *50*(12), 1819–1823. Retrieved 2022-09-19, from https://journals.ametsoc.org/view/journals/atsc/50/12/1520-0469_1993_050_1819_otrwsa_2_0_co_2.xml (Publisher: American Meteorological Society Section: Journal of the Atmospheric Sciences) doi: 10.1175/1520-0469(1993)050⟨1819:OTRWSA⟩2.0.CO;2

Rasch, P. J., Crutzen, P. J., & Coleman, D. B. (2008). Exploring the geoengineering of climate using stratospheric sulfate aerosols: The role of particle size. *Geophysical Research Letters*, *35*(2). Retrieved 2023-04-19, from https://onlinelibrary.wiley.com/doi/abs/10.1029/2007GL032179 (_eprint: https://onlinelibrary.wiley.com/doi/pdf/10.1029/2007GL032179) doi: 10.1029/2007GL032179

Rasmussen, E. N., & Blanchard, D. O. (1998, December). A Baseline Climatology of Sounding-Derived Supercell andTornado Forecast Parameters. *Weather and Forecasting*, *13*(4), 1148–1164. Retrieved 2023-01-17, from https://journals.ametsoc.org/view/journals/wefo/13/4/1520-0434_1998_013_1148_abcosd_2_0_co_2.xml (Publisher: American Meteorological Society Section: Weather and Forecasting) doi: 10.1175/1520-0434(1998)013⟨1148:ABCOSD⟩2.0.CO;2

Rasmussen, K. L., Prein, A. F., Rasmussen, R. M., Ikeda, K., & Liu, C. (2017, July). Changes in the convective population and thermodynamic environments in convection-permitting regional climate simulations over the United States. *Climate Dynamics*, *55*(1), 383–408. Retrieved 2022-05-12, from https://doi.org/10.1007/s00382-017-4000-7 doi: 10.1007/s00382-017-4000-7

Riahi, K., van Vuuren, D. P., Kriegler, E., Edmonds, J., O'Neill, B. C., Fujimori, S., ... Tavoni, M. (2017, January). The Shared Socioeconomic Pathways and their energy, land use, and greenhouse gas emissions implications: An overview. *Global Environmental Change*, *42*, 153–168. Retrieved 2023-01-23, from https://www.sciencedirect.com/science/article/pii/S0959378016300681 doi: 10.1016/j.gloenvcha.2016.05.009

Richter. (2022a). *Assessing Responses and Impacts of Solar climate intervention on the Earth system with stratospheric aerosol injection simulations (ARISE-SAI-1.5).* UCAR/NCAR - CISL - CDP. Retrieved 2023-07-14, from https://www.earthsystemgrid.org/dataset/id/29c8320f-c525-4cd2-8014-361eecec3907.html doi: 10.5065/9KCN-9Y79

Richter. (2022b). *CESM2-WACCM-SSP245 simulations.* UCAR/NCAR - CISL - CDP. Retrieved 2023-07-14, from https://www.earthsystemgrid.org/dataset/ucar.cgd.cesm2.waccm6.ssp245.html doi: 10.26024/0CS0-EV98

Richter, J., Visioni, D., MacMartin, D., Bailey, D., Rosenbloom, N., Lee, W., ... Lamarque, J.-F. (2022, April). *Assessing Responses and Impacts of Solar climate intervention on the Earth system with stratospheric aerosol injection (ARISE-SAI)* (preprint). Climate and Earth system modeling. Retrieved 2022-10-31, from https://egusphere.copernicus.org/preprints/2022/egusphere-2022-125/ doi: 10.5194/egusphere-2022-125

Rodgers, K. B., Lee, S.-S., Rosenbloom, N., Timmermann, A., Danabasoglu, G., Deser, C., ... Yeager, S. G. (2021, December). Ubiquity of human-induced changes in climate variability. *Earth System Dynamics*, *12*(4), 1393–1411. Retrieved 2022-05-12, from https://esd.copernicus.org/articles/12/1393/2021/ doi: 10.5194/esd-12-1393-2021

Sardeshmukh, P. D., & Hoskins, B. J. (1988, April). The Generation of Global Rotational Flow by Steady Idealized Tropical Divergence. *Journal of the Atmospheric Sciences*, *45*(7), 1228–1251. Retrieved 2022-09-19, from https://journals.ametsoc.org/view/journals/atsc/45/7/1520-0469_1988_045_1228_tgogrf_2_0_co_2.xml (Publisher: American Meteorological Society Section: Journal of the Atmospheric

Sciences) doi: 10.1175/1520-0469(1988)045⟨1228:TGOGRF⟩2.0.CO;2

Seeley, J. T., & Romps, D. M. (2015, March). The Effect of Global Warming on Severe Thunderstorms in the United States. *Journal of Climate*, *28*(6), 2443–2458. Retrieved 2023-03-30, from https://journals.ametsoc.org/view/journals/clim/28/6/jcli-d-14-00382.1.xml (Publisher: American Meteorological Society Section: Journal of Climate) doi: 10.1175/JCLI-D-14-00382.1

Sellar, A. A., Jones, C. G., Mulcahy, J. P., Tang, Y., Yool, A., Wiltshire, A., ... Zerroukat, M. (2019). UKESM1: Description and Evaluation of the U.K. Earth System Model. *Journal of Advances in Modeling Earth Systems*, *11*(12), 4513–4558. Retrieved 2023-03-24, from https://onlinelibrary.wiley.com/doi/abs/10.1029/2019MS001739 (_eprint: https://onlinelibrary.wiley.com/doi/pdf/10.1029/2019MS001739) doi: 10.1029/2019MS001739

Simpson, I. R., Tilmes, S., Richter, J. H., Kravitz, B., MacMartin, D. G., Mills, M. J., ... Pendergrass, A. G. (2019). The Regional Hydroclimate Response to Stratospheric Sulfate Geoengineering and the Role of Stratospheric Heating. *Journal of Geophysical Research: Atmospheres*, *124*(23), 12587–12616. Retrieved 2023-06-20, from https://onlinelibrary.wiley.com/doi/abs/10.1029/2019JD031093 (_eprint: https://onlinelibrary.wiley.com/doi/pdf/10.1029/2019JD031093) doi: 10.1029/2019JD031093

Smith, W., & Wagner, G. (2018, November). Stratospheric aerosol injection tactics and costs in the first 15 years of deployment. *Environmental Research Letters*, *13*(12), 124001. Retrieved 2023-05-23, from https://dx.doi.org/10.1088/1748-9326/aae98d (Publisher: IOP Publishing) doi: 10.1088/1748-9326/aae98d

Stroeve, J. C., Kattsov, V., Barrett, A., Serreze, M., Pavlova, T., Holland, M., & Meier, W. N. (2012). Trends in Arctic sea ice extent from CMIP5, CMIP3 and observations. *Geophysical Research Letters*, *39*(16). Retrieved 2023-01-20, from https://onlinelibrary.wiley.com/doi/abs/10.1029/2012GL052676 (_eprint: https://onlinelibrary.wiley.com/doi/pdf/10.1029/2012GL052676) doi: 10.1029/2012GL052676

Strzepek, K., Yohe, G., Neumann, J., & Boehlert, B. (2010, December). Characterizing changes in drought risk for the United States from climate change. *Environmental*

Research Letters, *5*(4), 044012. Retrieved 2023-01-20, from https://dx.doi.org/10.1088/1748-9326/5/4/044012 doi: 10.1088/1748-9326/5/4/044012

Taszarek, M., Allen, J. T., Groenemeijer, P., Edwards, R., Brooks, H. E., Chmielewski, V., & Enno, S.-E. (2020, December). Severe Convective Storms across Europe and the United States. Part I: Climatology of Lightning, Large Hail, Severe Wind, and Tornadoes. *Journal of Climate*, *33*(23), 10239–10261. Retrieved 2022-10-20, from https://journals.ametsoc.org/view/journals/clim/33/23/jcliD200345.xml (Publisher: American Meteorological Society Section: Journal of Climate) doi: 10.1175/JCLI-D-20-0345.1

Thompson, D. B., & Roundy, P. E. (2013, June). The Relationship between the Madden–Julian Oscillation and U.S. Violent Tornado Outbreaks in the Spring. *Monthly Weather Review*, *141*(6), 2087–2095. Retrieved 2023-05-22, from https://journals.ametsoc.org/view/journals/mwre/141/6/mwr-d-12-00173.1.xml (Publisher: American Meteorological Society Section: Monthly Weather Review) doi: 10.1175/MWR-D-12-00173.1

Tilmes, S., Richter, J. H., Kravitz, B., MacMartin, D. G., Mills, M. J., Simpson, I. R., ... Ghosh, S. (2018, November). CESM1(WACCM) Stratospheric Aerosol Geoengineering Large Ensemble Project. *Bulletin of the American Meteorological Society*, *99*(11), 2361–2371. Retrieved 2022-06-07, from https://journals.ametsoc.org/view/journals/bams/99/11/bams-d-17-0267.1.xml (Publisher: American Meteorological Society Section: Bulletin of the American Meteorological Society) doi: 10.1175/BAMS-D-17-0267.1

Tippett, M. K., Allen, J. T., Gensini, V. A., & Brooks, H. E. (2015, June). Climate and Hazardous Convective Weather. *Current Climate Change Reports*, *1*(2), 60–73. Retrieved 2023-01-24, from https://doi.org/10.1007/s40641-015-0006-6 doi: 10.1007/s40641-015-0006-6

Tippett, M. K., Lepore, C., & L'Heureux, M. L. (2022, September). Predictability of a tornado environment index from El Niño–Southern Oscillation (ENSO) and the Arctic Oscillation. *Weather and Climate Dynamics*, *3*(3), 1063–1075. Retrieved 2023-03-31, from https://wcd.copernicus.org/articles/3/1063/2022/ (Publisher: Copernicus GmbH) doi: 10.5194/wcd-3-1063-2022

Trapp, R. J., Diffenbaugh, N. S., Brooks, H. E., Baldwin, M. E., Robinson, E. D., & Pal,

J. S. (2007, December). Changes in severe thunderstorm environment frequency during the 21st century caused by anthropogenically enhanced global radiative forcing. *Proceedings of the National Academy of Sciences*, *104* (50), 19719–19723. Retrieved 2022-11-04, from https://www.pnas.org/doi/abs/10.1073/pnas.0705494104 (Publisher: Proceedings of the National Academy of Sciences) doi: 10.1073/pnas.0705494104

Trapp, R. J., Diffenbaugh, N. S., & Gluhovsky, A. (2009). Transient response of severe thunderstorm forcing to elevated greenhouse gas concentrations. *Geophysical Research Letters*, *36* (1). Retrieved 2023-02-07, from https://onlinelibrary.wiley.com/doi/abs/10.1029/2008GL036203 (_eprint: https://onlinelibrary.wiley.com/doi/pdf/10.1029/2008GL036203) doi: 10.1029/2008GL036203

Trapp, R. J., Hoogewind, K. A., & Lasher-Trapp, S. (2019, September). Future Changes in Hail Occurrence in the United States Determined through Convection-Permitting Dynamical Downscaling. *Journal of Climate*, *32* (17), 5493–5509. Retrieved 2023-03-31, from https://journals.ametsoc.org/view/journals/clim/32/17/jcli-d-18-0740.1.xml (Publisher: American Meteorological Society Section: Journal of Climate) doi: 10.1175/JCLI-D-18-0740.1

UNEP. (2022, October). Emissions Gap Report 2022: The Closing Window - Climate Crisis Calls for Rapid Transformation of Societies. Retrieved 2023-04-19, from https://wedocs.unep.org/xmlui/handle/20.500.11822/40874 (Accepted: 2022-10-19T13:29:26Z)

Visioni, D., Bednarz, E. M., Lee, W. R., Kravitz, B., Jones, A., Haywood, J. M., & MacMartin, D. G. (2023, January). Climate response to off-equatorial stratospheric sulfur injections in three Earth system models – Part 1: Experimental protocols and surface changes. *Atmospheric Chemistry and Physics*, *23* (1), 663–685. Retrieved 2023-02-13, from https://acp.copernicus.org/articles/23/663/2023/ (Publisher: Copernicus GmbH) doi: 10.5194/acp-23-663-2023

Visioni, D., MacMartin, D. G., Kravitz, B., Boucher, O., Jones, A., Lurton, T., ... Tilmes, S. (2021, July). Identifying the sources of uncertainty in climate model simulations of solar radiation modification with the G6sulfur and G6solar Geoengineering Model Intercomparison Project (GeoMIP) simulations. *Atmospheric Chemistry and Physics*, *21* (13), 10039–10063. Retrieved 2023-04-20, from https://acp.copernicus.org/articles/21/10039/2021/ (Publisher: Copernicus GmbH) doi: 10.5194/acp-21-10039-2021

Weisman, M. L., & Klemp, J. B. (1982, June). The Dependence of Numerically Simulated Convective Storms on Vertical Wind Shear and Buoyancy. *Monthly Weather Review*, *110*(6), 504–520. Retrieved 2023-01-24, from https://journals.ametsoc.org/view/journals/mwre/110/6/1520-0493_1982_110_0504_tdonsc_2_0_co_2.xml (Publisher: American Meteorological Society Section: Monthly Weather Review) doi: 10.1175/1520-0493(1982)110⟨0504:TDONSC⟩2.0.CO;2

Wilks, D. S. (2016, December). "The Stippling Shows Statistically Significant Grid Points": How Research Results are Routinely Overstated and Overinterpreted, and What to Do about It. *Bulletin of the American Meteorological Society*, *97*(12), 2263–2273. Retrieved 2023-06-20, from https://journals.ametsoc.org/view/journals/bams/97/12/bams-d-15-00267.1.xml (Publisher: American Meteorological Society Section: Bulletin of the American Meteorological Society) doi: 10.1175/BAMS-D-15-00267.1

Zarnetske, P. L., Gurevitch, J., Franklin, J., Groffman, P. M., Harrison, C. S., Hellmann, J. J., . . . Yang, C.-E. (2021, April). Potential ecological impacts of climate intervention by reflecting sunlight to cool Earth. *Proceedings of the National Academy of Sciences*, *118*(15), e1921854118. Retrieved 2023-04-19, from https://www.pnas.org/doi/full/10.1073/pnas.1921854118 (Publisher: Proceedings of the National Academy of Sciences) doi: 10.1073/pnas.1921854118

Supporting Information for "Assessing the impact of stratospheric aerosol injection on U.S. convective weather environments"

Ivy Glade[1], James W. Hurrell[1], Lantao Sun[1], Kristen L. Rasmussen[1]

[1]Department of Atmospheric Science, Colorado State University, Fort Collins, CO, USA

Contents of this file

1. Figures S1 to S4

Introduction The supporting information file contains figures S1-S4 which support results and discussion in the main manuscript.

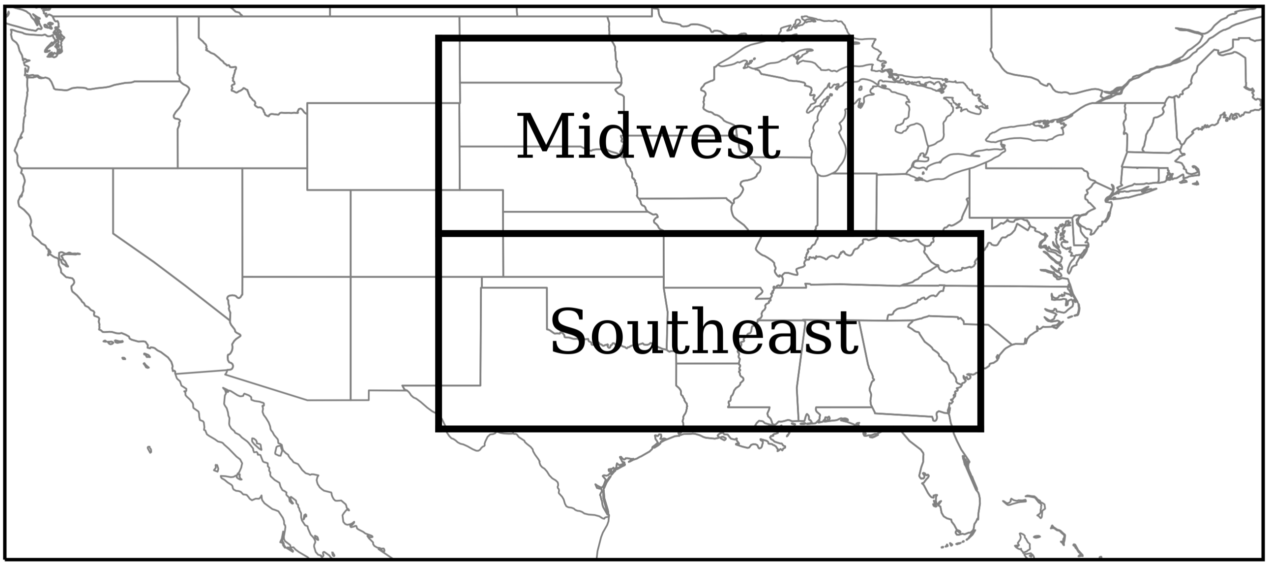

Figure S1. The Midwest and Southeast regions. The Midwest is defined by the grid points bounded by 30°-39°N and 255°-280°W. The Southeast is defined by the grid points bounded by 39°-48°N and 255°-274°W.

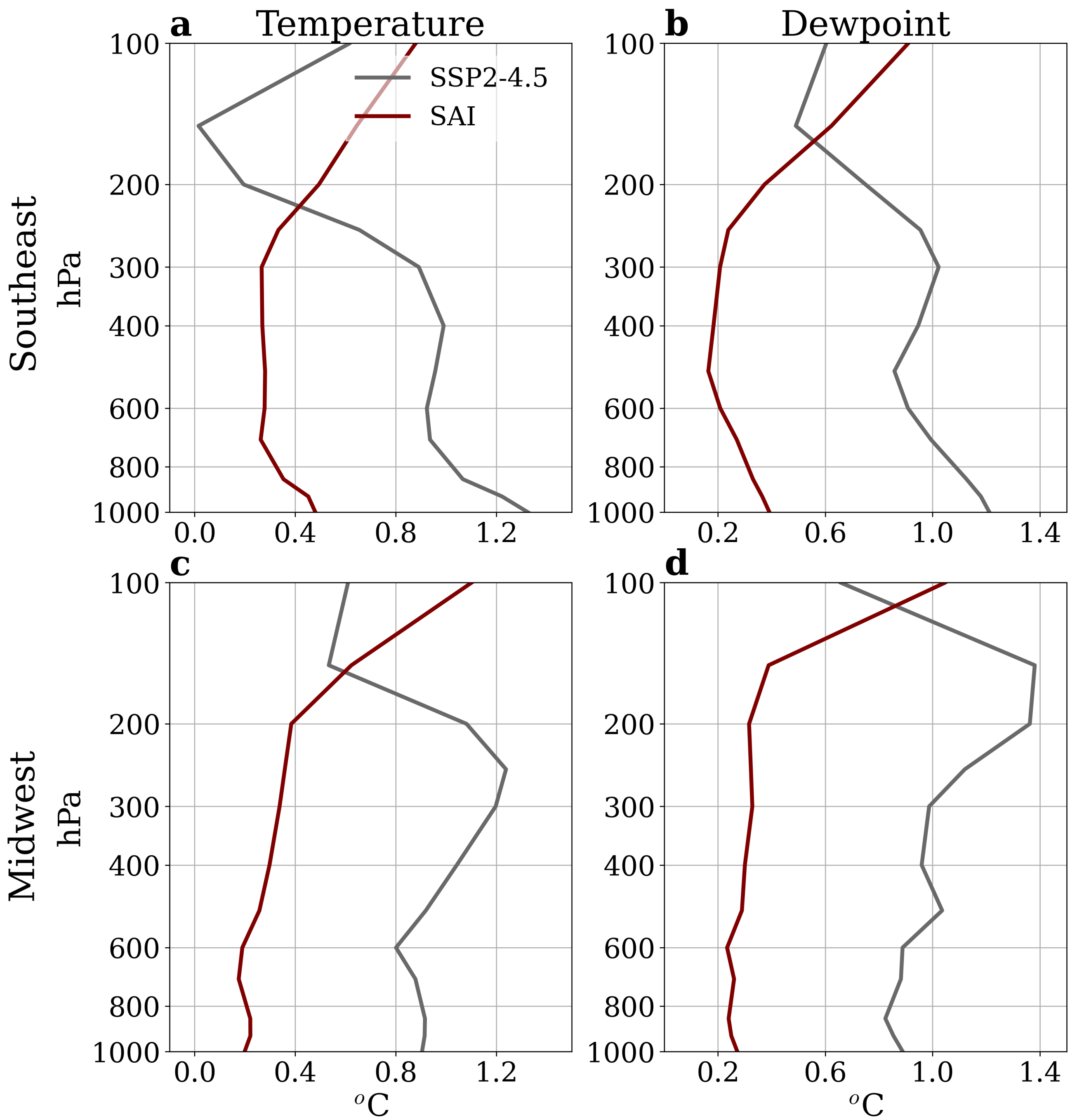

Figure S2. Ensemble mean changes in the vertical profiles of temperature (a and c) and dew point (b and d) over the Southeast in MAM and the Midwest in JJA for 2060-2069 relative to 2015-2034. The SSP2-4.5 simulations are shown in gray and the SAI simulations are shown in red.

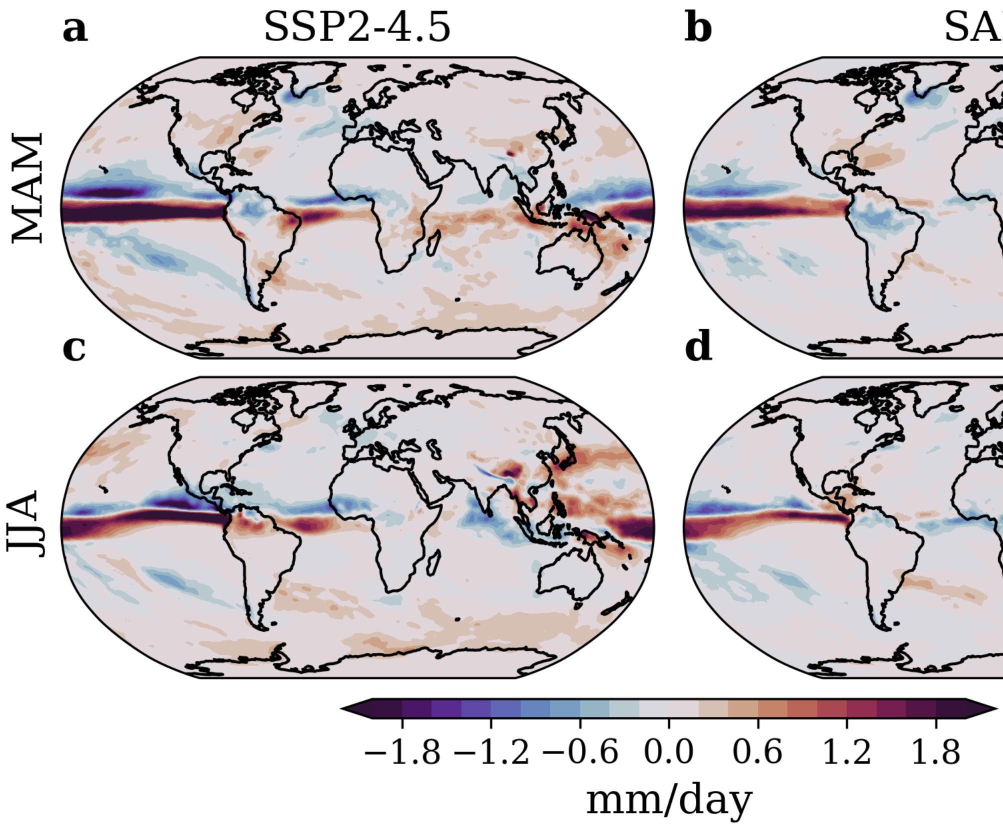

Figure S3. Ensemble mean change in precipitation (2060-2069 relative to 2015-2034) for the SSP2-4.5 and SAI simulations during the boreal spring and summer seasons.

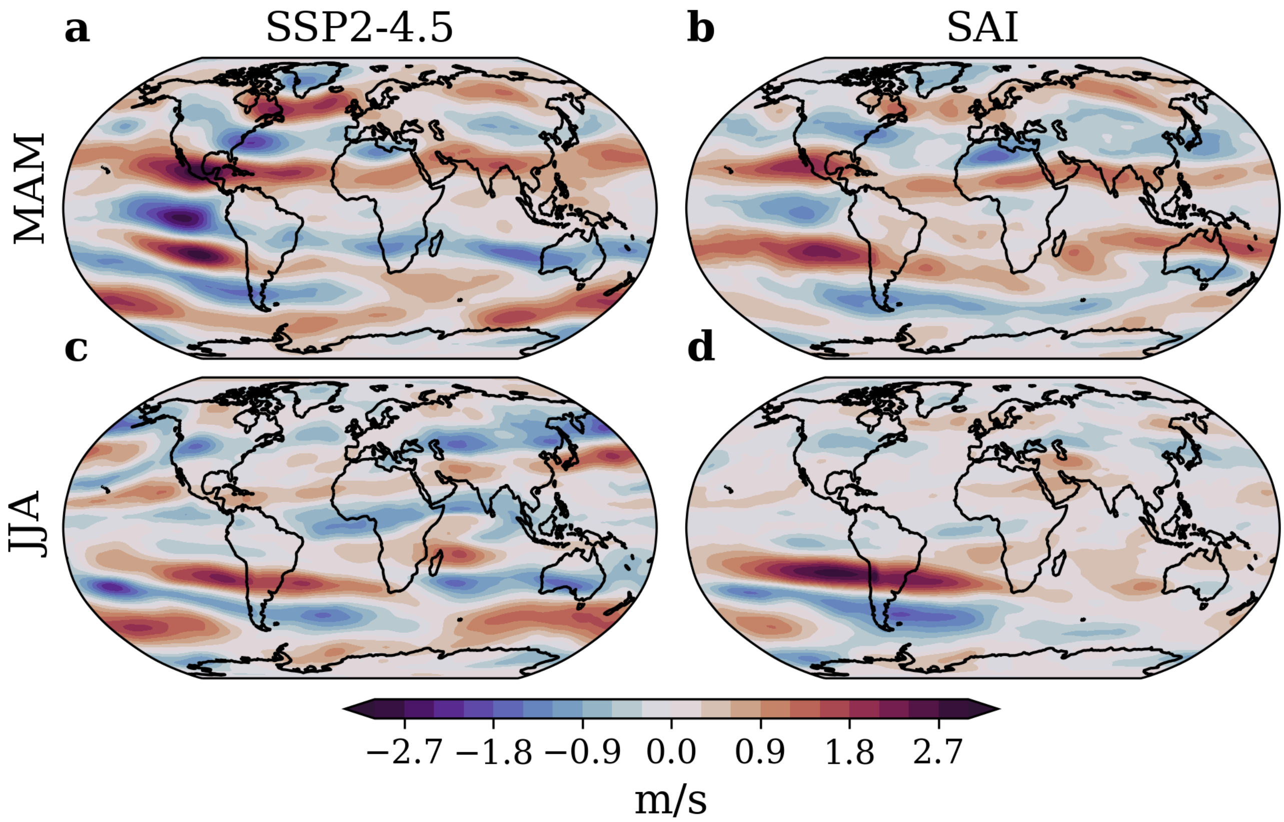

Figure S4. Ensemble mean change in 300 hPa wind speed (2060-2069 relative to 2015-2034) for the SSP2-4.5 and SAI simulations during the boreal spring and summer seasons.